

GIBBS PHENOMENON FOR DISPERSIVE PDES

GINO BIONDINI AND THOMAS TROGDON

ABSTRACT. We investigate the Cauchy problem for linear, constant-coefficient evolution PDEs on the real line with discontinuous initial conditions (ICs). First, we establish sufficient conditions for any given order of differentiability of the solution for positive times. Importantly, these conditions allow for jump discontinuities in the IC. Second, we characterize the small-time behavior of the solution near such discontinuities, and we show that the leading-order solution near a discontinuity is given by a similarity solution expressed in terms of special functions which are generalizations of the classical special functions. Third, we present an efficient numerical method for the accurate evaluation of these special functions. Finally, we show that the leading-order behavior of the solution of dispersive PDEs near a discontinuity of the ICs is characterized by Gibbs-type oscillations, and we prove that, asymptotically, the overshoot of the solution near the discontinuity coincides exactly with the Wilbraham-Gibbs constant.

1. Introduction

The Gibbs phenomenon is the well-known behavior of the Fourier series of a piecewise continuously differentiable periodic function at a jump discontinuity. Namely, the partial sums of the Fourier series have large oscillations near the jump, which typically increase the maximum of the sum above that of the function itself [5, 20]. Moreover, the overshoot does not subside as the frequency increases, but instead approaches a finite limit. The Gibbs phenomenon is typically viewed as a numerical artifact in the numerical representation of a function due to truncation. Here we view the Gibbs phenomenon as a product of *non-uniform convergence*. Namely, the partial sums of the Fourier series are analytic and converge (in an appropriate sense) to a discontinuous function, and hence, convergence must be non-uniform in any neighborhood of the discontinuity. In turn, this gives rise to highly oscillatory behavior. Keeping this view of the Gibbs phenomenon in mind, we show in this work that *the solution of dispersive PDEs with discontinuous initial conditions (ICs) exhibit real Gibbs-like behavior for short times*. E.g., Fig. 1.1 shows a solution of (1.1) with $\omega(k) = k^5$ for small times.

Specifically, we consider initial value problems (IVPs) of the form

$$(1.1) \quad iq_t - \omega(-i\partial_x)q = 0,$$

with $\omega(k) = \omega_n k^n + O(k^{n-1})$ and with IC

$$(1.2) \quad q(x, 0) = q_o(x)$$

lying in an appropriate function space. (Precise requirements will be given later.) It is well known that, for hyperbolic PDEs, the discontinuities of the IC travel along characteristics (weak solutions) [7, 14]. For dispersive and diffusive PDEs, in contrast, even if the ICs are discontinuous, the solution of the IVP is typically classical $\forall x \in \mathbb{R}$ for all $t > 0$ as long as the IC has sufficient decay as $|x| \rightarrow \infty$. But an obvious question is: *What does the solution actually look like?* Answering this question is useful for many reasons. For example: (i) to evaluate asymptotics for linear and nonlinear problems [39], (ii) to build/test numerical integrators, and (iii) to understand the behavior of initial boundary value problems (IBVPs) (see below). Surprisingly, however, while the smoothing effects of diffusion are well known, this perspective on dispersive regularization is not as well characterized in the literature to the best of our knowledge.

Let us briefly elaborate on item (iii) above. One of the original motivations for this work was the study of corner singularities in IBVPs [4, 15, 16, 17]. The issue at hand is the following. Consider (1.1), with $n = 2$, posed on the domain $D = (0, \infty) \times (0, T)$ so that one has to also specify boundary data at $x = 0$, say $q(0, t) = g_0(t)$. The smoothness of $q(x, t)$ in \bar{D} is restricted not only by the smoothness (and decay) of $q_o(x)$ and $g_0(t)$ but by the compatibility of these two functions at $x = t = 0$, i.e., to first-order, $q_o(0) = g_0(0)$. (Higher-order conditions are found by enforcing the PDE holds at the corner of the domain.) When compatibility fails at some order, a corner singularity is present. One would obviously like to characterize the effect of such a corner singularity on the solution of an IBVP. It soon became clear, however, that in order to do so, one needs to fully understand the behavior of IVPs with discontinuous ICs.

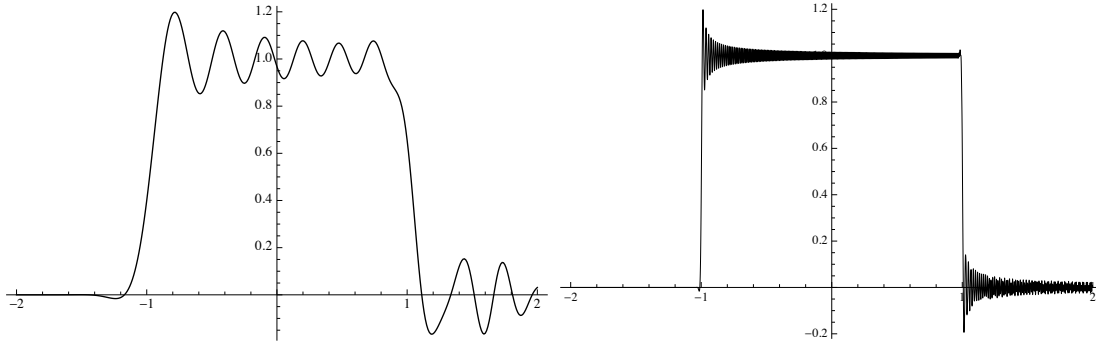


Figure 1.1: The solution of (1.1) with $\omega(k) = k^5$ and IC $q_o(x) = 1$ if $|x| \leq 1$ and $q_o(x) = 0$ otherwise. Left: $t = 10^{-6}$. Right: $t = 10^{-12}$. The solution exhibits the Gibbs phenomenon, as discussed in detail in Section 4.

Technical conditions aside, if a function $f(x)$ is discontinuous, its Fourier transform $\hat{f}(k)$ exhibits slow decay as $k \rightarrow \infty$. More precisely, if $f^{(n)}(x)$ is discontinuous then $\hat{f}(k) = O(1/k^{n+1})$ as $k \rightarrow \infty$. One of the central messages of this work is that: *The slow decay of the Fourier transform of q_o as $k \rightarrow \infty$ affects the short-time asymptotics of the solution $q(x, t)$.*

The outline of this work is the following. In Section 2 we discuss classical results concerning the well-posedness of the IVP for (1.1) and the smoothness of its solutions. In the same section we also state sufficient conditions for the solution to be differentiable at any given order when $t > 0$. Proceeding, in Section 3 we perform the asymptotic analysis in the case of a single discontinuity in the IC q_o . There we identify the special functions that describe the Gibbs-like behavior. Such functions are generalizations of the classical special functions, and are computable with similar numerical methods. In Section 4 we display some sample solutions, we discuss their Gibbs-like behavior, we further study the properties of the special functions and we establish a precise connection with the classical Gibbs phenomenon. In Section 5 we treat the case where q'_o has one jump discontinuity. In Section 6 we present our general result, which allows for multiple discontinuities in q_o itself or in any of its derivatives. A full asymptotic expansion is derived near, and away from, the singular (i.e., non-smooth) points of q_o . Section 7 contains additional details on the analysis and numerical computation of the special functions considered here. Finally, Section 8 concludes this work with a discussion of the results and some final remarks.

Further details and technical results are relegated to four appendices. In Appendix A we review some well-known results about well-posedness of the IVP. In Appendix B we prove the result (stated in Section 2) concerning the classical smoothness of the solution for $t > 0$, using the method of steepest descent for integrals. Appendix C contains technical results for determining the order of the error terms in our short-time expansions. Finally, in Appendix D we study the robustness of the Gibbs phenomenon by analyzing the behavior of solutions whose ICs are a small perturbation of a discontinuous function.

The function $\omega(k)$ is referred to as the *dispersion relation* of the PDE (1.1). Throughout this work, we will take the dispersion relation $\omega(k)$ to be polynomial. Note that one can always remove constant and linear terms from $\omega(k)$ by performing a phase rotation and a Galilean transformation, respectively. That is, without loss of generality one can take

$$(1.3) \quad \omega(k) = \sum_{j=2}^n \omega_j k^j.$$

We will assume that this has been done throughout this work.

2. Regularity results for linear evolution PDEs

We begin by briefly reviewing some results regarding the solution of IVPs for linear PDEs of the form (1.1), recalling concepts about types of solutions and existence and uniqueness. We define the Fourier transform pair for $f \in L^2(\mathbb{R})$

by

$$(2.1) \quad \hat{f}(k) = \int_{-\infty}^{\infty} e^{-ikx} \hat{f}(x) dx, \quad f(x) = \frac{1}{2\pi} \int_{-\infty}^{\infty} e^{ikx} \hat{f}(k) dk.$$

Throughout, we use the caret ($\hat{\cdot}$) to denote the spatial Fourier transform.

Definition 2.1. The function $q(x, t)$ is a classical solution of the PDE (1.1) with (1.3) in an open region $\Omega \subset \mathbb{R}^2$ if all derivatives present in the PDE exist for all $(x, t) \in \Omega$ and the PDE is satisfied pointwise.

Recall that $\omega(k)$ needs to satisfy certain conditions in order for the IVP for (1.1) to be well posed. Specifically, it is straightforward to see that $\text{Im}[\omega(k)]$ must be bounded from above. Letting $n = \deg[\omega(k)]$ this condition implies $\text{Im} \omega_n \leq 0$ if n is even and $\omega_n \in \mathbb{R}$ if n is odd. Throughout the manuscript, we reserve n for the order of the dispersion relation. Also recall that the PDE is said to be dispersive if $\omega''(k) \neq 0$ [41].

Definition 2.2. A function $q(x, t)$ is a weak solution of (1.1) with (1.3) in an open region Ω if

$$(2.2) \quad L_\omega[q, \phi] = \int_{\Omega} q(x, t)(-i\partial_t \phi(x, t) - \omega(i\partial_x) \phi(x, t)) dx dt = 0,$$

for all $\phi \in C_c^\infty(\Omega)$ (with the subscript c denoting compact support).

Definition 2.3. A function $q(x, t)$ is an L^2 solution of the IVP for (1.1) with dispersion relation (1.3) and IC (1.2) if: (i) $q \in C^0([0, T]; L^2(\mathbb{R}))$, (ii) q satisfies (2.2) with $\Omega = \mathbb{R} \times \mathbb{R}^+$, and (iii) $q(\cdot, 0) = q_o$ a.e.

Let us recall some well-known facts, whose proofs are reviewed in Appendix A. The function $q(x, t)$ defined by the Fourier transform reconstruction formula

$$(2.3) \quad q(x, t) = \frac{1}{2\pi} \int_{\mathbb{R}} e^{i\theta(x, t, k)t} \hat{q}_o(k) dk, \quad \hat{q}_o(k) = \int_{\mathbb{R}} e^{-ikx} q_o(x) dx,$$

with

$$(2.4) \quad \theta(x, t, k) = kx - \omega(k)t,$$

is the unique L^2 solution of the IVP provided the imaginary part of $\omega(k)$ is bounded above and $q_o \in L^2(\mathbb{R})$. Moreover, the solution, as a function in $C^0([0, T]; L^2(\mathbb{R}))$ depends continuously on the initial data.

Assuming that we have a well-posed IVP and a well-defined solution formula, the remainder of this section, and most of the remainder of the manuscript, is devoted to discussing properties of the L^2 solution $q(x, t)$. Two properties can be readily seen:

1. $q(\cdot, t) \rightarrow q(\cdot, 0)$ in $L^2(\mathbb{R})$ as $t \downarrow 0$,
2. if $q_o \in H^1(\mathbb{R})$ then $q(\cdot, t) \rightarrow q(\cdot, 0)$ uniformly as $t \downarrow 0$.

More delicate questions can be asked about pointwise behavior in the short-time limit, however. In particular, Sjölin [35] showed that when $\omega(k) = k^{2m}$, $m = 1, 2, \dots$, and $q_o \in H^s(\mathbb{R})$ with compact support for $s \geq 1/4$, $\lim_{t \downarrow 0} q(x, t) = q(x, 0)$ for a.e. $x \in \mathbb{R}$. This result was generalized in [27] for general $\omega(k)$ without the assumption of compact support. (See also [31, 37, 40].) The results that follow will only demonstrate a.e. convergence for a subset of $H^{1/4}(\mathbb{R})$. On the other hand, the short-time expansion that we will provide in the following sections is new.

Interesting questions related to the regularity of the solution can also be asked. As is noted in [36], when $\omega(k) = k^2, k^3$ the solutions are easily seen to be continuous for $t > 1$ provided $q \in L^2 \cap L^1(\mathbb{R})$. Furthermore the $L^\infty(\mathbb{R})$ norm of $q(\cdot, t)$ decays in time. A Strichartz-type result was provided in [27] showing, in particular, the space-time estimate $\|q\|_{L^8(\mathbb{R}^2)} \leq C\|q_o\|_{L^2(\mathbb{R})}$ for $\omega(k) = k^3$.

In Appendix 2 we prove results of a classical nature concerning the regularity of the solution. In particular, the following results are proved:

Theorem 2.4. Let $\omega(k)$ be as in (1.3) and $q(x, t)$ as in (2.3), with $q_o \in L^2(\mathbb{R}) \cap L^1(\mathbb{R}, (1 + |x|)^\ell dx)$.

(i) If

$$\ell \geq \frac{2m - n + 2}{2(n - 1)},$$

$q(x, t)$ is differentiable m times with respect to x for $t > 0$.

(ii) If

$$\ell \geq \frac{2jn - n + 2}{2(n-1)},$$

$q(x, t)$ is differentiable j times with respect to t for $t > 0$.

Corollary 2.5. Under the same hypotheses as in Theorem 2.4, if

$$\ell \geq \mathfrak{C}_n \triangleq \frac{n+2}{2(n-1)},$$

the L^2 solution of the IVP is classical for $t > 0$.

3. Short-time asymptotics: discontinuous ICs

Recall that the above representation for the weak solution (2.3) of the IVP is valid as long as the IC $q_o(x)$ belongs to $L^2(\mathbb{R})$. We first consider initial data with a single discontinuity. For now we will assume that q_o satisfies the following properties:

Assumption 3.1. Let

- $q_o \in L^2(\mathbb{R})$,
- $[q_o(c)] \triangleq q_o(c^+) - q_o(c^-) \neq 0$,
- q'_o exists on $(-\infty, c) \cup (c, \infty)$,
- $q'_o \in L^q(-\infty, c) \cap L^q(c, \infty)$ for some $1 < q < \infty$, and
- q_o is compactly supported.

In later sections we will discuss the effect of discontinuities in the derivatives of the IC and we will remove the condition of compact support. The phenomenon we wish to investigate here is the following. The solution is classical for $t > 0$, but converges to a discontinuous function as $t \rightarrow 0$. Thus, the limit generally exists in $L^2(\mathbb{R})$ but must fail to be uniform. We next derive an expansion that characterizes the behavior of the solution near this discontinuity for short times.

To derive this expansion, it is convenient to integrate the definition (2.1) of the Fourier transform by parts:

$$(3.1) \quad \hat{q}_o(k) = \left(\int_{-\infty}^c + \int_c^{\infty} \right) e^{-ikx} q_o(x) dx = \frac{1}{ik} e^{-ikc} [q_o(c)] + \frac{1}{ik} F(k),$$

where

$$(3.2) \quad F(k) = \left(\int_{-\infty}^c + \int_c^{\infty} \right) e^{-ikx} q'_o(x) dx, \quad [q_o(c)] = q_o(c^+) - q_o(c^-).$$

In Appendix C we discuss the properties of $F(k)$. Note that both terms in the right-hand side (RHS) of (3.1) are singular at $k = 0$, but their sum $\hat{q}_o(k)$ is not. Inserting (3.1) in the reconstruction formula (2.1) for the solution of the IVP yields:

$$(3.3) \quad q(x, t) = \frac{1}{2\pi} [q_o(c)] \oint_{\mathbb{R}} e^{i(k(x-c)-\omega(k)t)} \frac{dk}{ik} + \frac{1}{2\pi} \oint_{\mathbb{R}} e^{i\theta(x,t,k)} F(k) \frac{dk}{ik}.$$

where \oint denotes the principal value (p.v.) integral. The principal value sign is now needed because each of the integrands in (3.3) is separately singular at $k = 0$. Of course, one could have chosen other ways to regularize the singularity, and the final result for $q(x, t)$ is independent of this choice.

We next show that the second term in the RHS of (3.3) is continuous as a function of x for all $t \geq 0$, while the first term yields the dominant behavior in the neighborhood of the discontinuity at small times. More precisely, we can write the p.v. integral in (3.3) as:

$$(3.4) \quad \oint_{\mathbb{R}} f(k) dk = \int_C f(k) dk + \pi i \operatorname{Res}[f(k)]_{k=0}$$

where C is the contour shown in Fig. 3.1. Define

$$(3.5) \quad I_{\omega,0}(y, t) \triangleq \frac{1}{2\pi} \int_C e^{i[ky-\omega(k)t]} \frac{dk}{ik}.$$

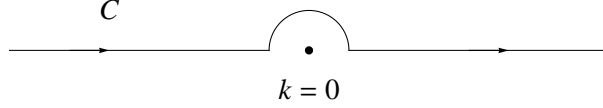


Figure 3.1: The integration contour C for the evaluation of the principal value integral in (3.4). We assume the radius of the semi-circle is less than 1.

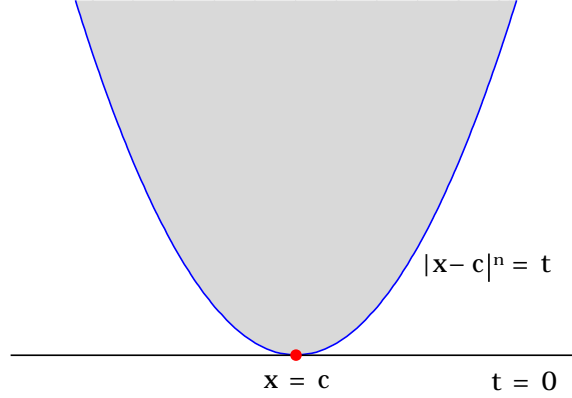


Figure 3.2: The regularization region (in gray) around a discontinuity in the IC.

(The reason for the subscript “0” will become apparent later on when we generalize these results to discontinuities in the higher derivatives.) Also, define

$$q_c = \frac{1}{2} [q_o(c)] + \frac{1}{2\pi} \oint_{\mathbb{R}} e^{ikc} F(k) \frac{dk}{ik}, \quad q_{\text{res}}(y, t) = \frac{1}{2\pi} \int_{\mathbb{R}} e^{ikc} \frac{e^{i\theta(y,t,k)} - 1}{ik} F(k) dk.$$

Recalling $\text{Res}_{k=0}(e^{i\theta(x-c,t,k)}/k) = 1$, we then write the decomposition (3.3) as

$$(3.6) \quad q(x, t) = q_c + [q_o(c)] I_{\omega,0}(x - c, t) + q_{\text{res}}(x - c, t).$$

Note that the principal value is not needed on $q_{\text{res}}(y, t)$, because the integrand is continuous at $k = 0$. Note also that the above decomposition holds for an arbitrary dispersion relation $\omega(k)$.

Importantly, each of the three terms in (3.6) are individually a solution of the PDE (1.1). However, each of them provides a different type of contribution. Indeed, a closer look allows the following interpretation of these pieces:

- (i) q_c represents a constant offset.
- (ii) $[q_o(c)] I_{\omega,0}(y, t)$ characterizes the dominant behavior near the jump discontinuity. The detailed properties of $I_{\omega,0}(y, t)$ are discussed in Appendix B. In particular, Theorem B.6 implies

$$(3.7) \quad \lim_{y \rightarrow \infty} I_{\omega,0}(y, t) = 0, \quad \lim_{y \rightarrow -\infty} I_{\omega,0}(y, t) = -1.$$

Note also that $\lim_{t \downarrow 0} I_{\omega,0}(0, t) \neq 0$.

- (iii) $q_{\text{res}}(c, 0) = 0$, and $q_{\text{res}}(x, t)$ is Hölder continuous and vanishes at $(x, t) = (c, 0)$ for $t \geq 0$.

One can look at the last item essentially as a trivial consequence of the first two, because the offset value and the jump behavior are all captured by the first and second contribution, respectively. In practice, however, the proof is done in the reverse. Namely, in Appendix C we prove (iii) and we obtain precise estimates for the behavior of $q_{\text{res}}(x - c, t)$ near $(x, t) = (c, 0)$. More precisely, we show that, for $\|F\|_{L^p(\mathbb{R})} < \infty$,

$$(3.8) \quad q_{\text{res}}(x - c, t) = O(|x - c|^{1/p} + |t|^{1/(np)}).$$

The error term in the above short-time expansion is consistent as $t \rightarrow 0$ as long as $|x - c|^n = O(t)$. That is, the above expansion is valid in the region $|x - c|^n \leq Ct$ (for some $C > 0$) in the neighborhood of a discontinuity c . We call such region the *regularization region*. Such a region is illustrated in Figure 3.2.

One may also wish to understand the behavior of the solution in the short-time limit away from the singularity. Of course, to leading order, we expect it to be unaffected by the singularity and to limit pointwise to the IC. To prove that this is indeed the case, one must derive an estimate for the error term. The asymptotics of $I_{\omega,m}(x - c, t)$ can be fully characterized, see Theorem B.6. The relevant behavior for the present purposes is

$$I_{\omega,0}(x - c, t) = -\chi_{(-\infty,0)}(x - c) + \mathcal{O}(t^{1/(2(n-1))})$$

as $t \rightarrow 0$ uniformly in the region $|x - c| \geq \delta > 0$. Here and below, $\chi_R(y)$ is the characteristic function of a set R . (Namely, $\chi_R(y) = 1$ for $y \in R$ and $\chi_R(y) = 0$ otherwise.) We then have

$$q(x, t) = [q_o(c)](\frac{1}{2} - \chi_{(-\infty,0)}(x - c)) + \frac{1}{2\pi} \oint_{\mathbb{R}} e^{i\theta(x,t,k)} F(k) \frac{dk}{ik} + \mathcal{O}(t^{1/(2(n-1))}).$$

The relevant tool for the characterizing the limiting behavior of the rest of the solution is Lemma C.1. From that result, (3.1) and the above discussion it follows that

$$q_0(x) = [q_o(c)](\frac{1}{2} - \chi_{(-\infty,0)}(x - c)) + \frac{1}{2\pi} \oint_{\mathbb{R}} e^{ikx} F(k) \frac{dk}{ik}.$$

Therefore, for $|s - c| \geq \delta > 0$ and $\|F\|_{L^p(\mathbb{R})} < \infty$, we have

$$(3.9) \quad q(x, t) = q_0(s) + \mathcal{O}(|x - s|^{1/p} + |t|^{1/(np)} + |t|^{1/(2(n-1))}).$$

These observations also allow us to prove the following universality theorem:

Theorem 3.1. *Under the conditions of Assumption 3.1,*

$$\lim_{t \downarrow 0} \frac{q(c + x|\omega_n t|^{1/n}, t) - q_c}{[q_o(c)]} = I_{\omega_n,0}(x, 1), \quad \omega_n(k) = \arg(\omega_n)k^n,$$

uniformly for x in a bounded set.

Proof. The equality

$$\lim_{t \downarrow 0} \frac{q(c + x|\omega_n t|^{1/n}, t) - q_c}{[q_o(c)]} = \lim_{t \downarrow 0} I_{\omega_n,0}(x|\omega_n|^{1/n} t^{1/n}, t),$$

follows directly from (3.8). Then

$$I_{\omega_n,0}(x|\omega_n|^{1/n} t^{1/n}, t) = \frac{1}{2\pi} \int_C e^{i(k|\omega_n|^{1/n} t^{1/n})x - i \arg(\omega_n)(|\omega_n|^{1/n} k t^{1/n})^n - r(k)t} \frac{dk}{ik},$$

where $r(k)$ is a polynomial of degree at most $n - 1$. Using $kt^{1/n}|\omega_n|^{1/n} \mapsto k$, and redefining C , we have

$$I_{\omega_n,0}(x|\omega_n|^{1/n} t^{1/n}, t) = \frac{1}{2\pi} \int_C e^{ikx - i \arg(\omega_n)k^n - r(k|\omega_n|^{-1/n} t^{-1/n})t} \frac{dk}{ik}.$$

But $r(k|\omega_n|^{-1/n} t^{-1/n})t \rightarrow 0$ as $t \rightarrow 0$. To see that the limit can be passed inside the integral, deform C so that it passes along the steepest descent paths of $e^{-i\omega_n k}$, then pass the limit inside using the dominated convergence theorem and deform back to C . From this the result follows. \square

This is interpreted as a universality theorem because, after proper rescaling, the solution is the same independent of both the initial condition and the lower terms in the dispersion relation. Such a statement also holds near each discontinuity when there is finitely many such discontinuities, see Section 6.

4. Gibbs phenomenon for dispersive PDEs

We now discuss the implications of decomposition (3.6) regarding the behavior of the solution of the IVP in the short time limit.

We have seen that, apart from a constant offset, the dominant behavior of the solution in the regularization region near a discontinuity of the IC is provided by the function $I_{\omega,0}(y, t)$. In this section we therefore examine more closely the properties of such functions. We start by discussing a few simple examples.

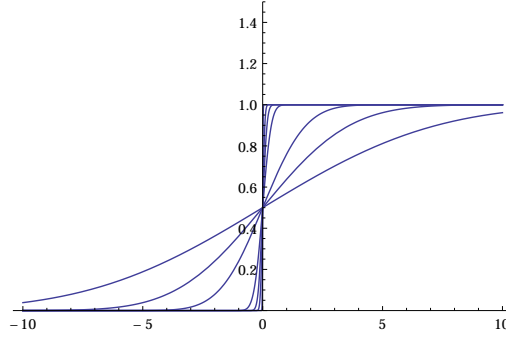


Figure 4.1: The integral $I_0(x, t) + 1$ (vertical axis) as a function of x (horizontal axis) for the heat equation (4.1) at various values of time: $t = 0.01, 0.05, 0.1, 0.2, 1, 2$, and 4 .

Example 1: Heat equation. Consider the PDE

$$(4.1) \quad q_t = q_{xx},$$

corresponding to $\omega(k) = -ik^2$. Let $s = y/t^{1/2}$ and $\lambda = kt^{1/2}$. Then

$$(4.2) \quad I_{\text{heat},0}(y, t) = \frac{1}{2\pi} \int_C e^{i\lambda s - \lambda^2} \frac{d\lambda}{i\lambda} = \frac{1}{2} (\text{erf}(s/2) - 1),$$

where with some abuse of notation we write $I_{\text{heat},0}(s, t) = I_{\text{heat},0}(y(s), t)$. Note that an easy way to compute the above integral is by using the relation

$$(4.3) \quad \frac{d}{ds} I_{\text{heat},0}(s, t) = \frac{1}{2\pi} \int_C e^{i\lambda s - \lambda^2} d\lambda = \frac{1}{2\sqrt{\pi}} e^{-s^2/4},$$

We will see a generalization of (4.3) later.

Figure 4.1 shows the value of $I_0(x, t)$ as a function of x at different times. The resulting effect is that of a diffusion-induced smoothing of the initial discontinuity. This behavior is well-known, and is discussed in most classical PDE books [14]. What is perhaps less known, however, is the counterpart of this behavior for dispersive PDEs, which we turn to next.

Example 2: Schrödinger equation. Consider now the free-particle, one-dimensional linear Schrödinger equation, namely,

$$(4.4) \quad iq_t + q_{xx} = 0,$$

corresponding to $\omega(k) = k^2$. In this case,

$$(4.5) \quad I_{\text{schr},0}(y, t) = \frac{1}{2\pi i} \int_C e^{i\lambda s - i\lambda^2} \frac{d\lambda}{\lambda} = \frac{1}{2} (\text{erf}(e^{-i\pi/4} s/2) - 1).$$

(The integral is evaluated in a similar way as before, but now a $\pi/4$ rotation of the contour in the complex plane is needed to get a closed-form expression.)

The corresponding behavior is shown in Fig. 4.2. For both PDEs, the dominant behavior near the discontinuity is expressed in terms of a *similarity solution*, depending on x and t only through the similarity variable $s = (x - c)/t^{1/2}$. We will see later that this is in fact a general feature for PDEs with monomial dispersion relations. The solution behavior however is very different: While for the heat equation the integral $I_{\omega,0}(x, t)$ captures the smoothing effect of the PDE, for the Schrödinger equation, $I_{\omega,0}(x, t)$ results in oscillations.

Another difference between the two PDEs is that, for the Schrödinger equation, $I_{\omega,0}(y, t)$ is complex-valued for real values of y [unlike the corresponding integral for the heat equation]. As a result, the behavior of the absolute value of the solution is offset-dependent, as demonstrated in Fig. 4.2. That is, the absolute value of the full solution of the PDE can in general display an interference pattern between $I_{\text{schr},0}(y, t)$ and the constant offset.

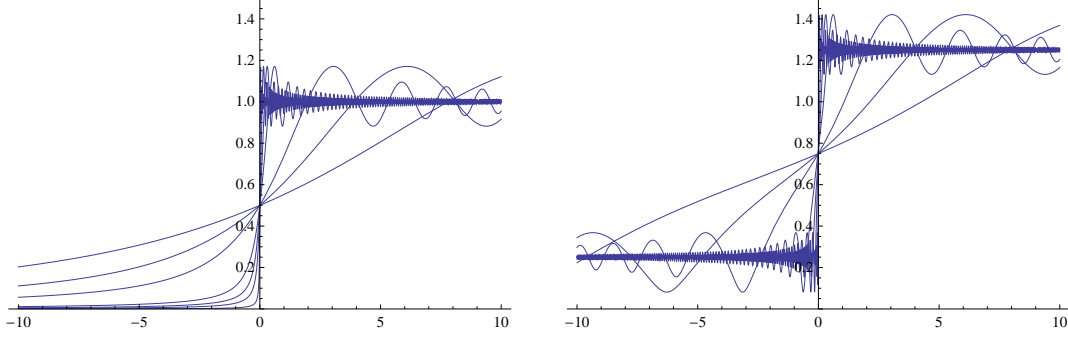


Figure 4.2: Left: Absolute value $|I_0(x, t) + 1|$ as a function of x for the Schrödinger equation (4.4) at the same values of t as in Fig. 4.1. Right: Same for $|I_0(x, t) + \frac{5}{4}|$. Note in this last case the presence of oscillations to the left of the jump.

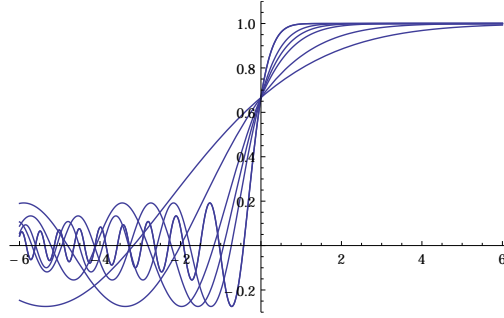


Figure 4.3: Same as Fig. 4.1, but for the Stokes equation (4.6).

Gibbs-like oscillations of dispersive PDEs. The solution of the Schrödinger equation described above shares the three defining features of the Gibbs phenomenon, namely: (i) non-uniform convergence of the solution of the PDE to the IC as $t \downarrow 0$ in a neighborhood of the discontinuity; (ii) spatial oscillations with increasing (in fact, unbounded) frequency as $t \downarrow 0$ (because they are governed by the similarity variable); (iii) constant overshoot in a neighborhood of the discontinuity as $t \downarrow 0$. (We will elaborate on this last issue later in the section.) Thus, the limit $t \downarrow 0$ for the solution of the PDE is perfectly analogous to the limit $n \rightarrow \infty$ in the truncation of the Fourier series.

These results are not limited to (4.4), but rather are a general feature of dispersive PDEs with discontinuous ICs. [Recall that in Section 3 we already showed that the short-time asymptotic expansion of the solution holds for all dispersive PDEs of the form (1.1).] Thus, *the Gibbs-like oscillations represent the real behavior of the solution of dispersive PDEs, and are not a numerical artifact.* In other words, Fig. 4.2 (as well as Fig. 4.3 and the figures in Section 7) are not a result of truncation error! We believe that this fact has important consequences for the numerical solution of dispersive PDEs, particularly, in finite-volume methods where a so-called Riemann problem must be solved.

Example 3: Stokes equation. Consider now the Stokes equations

$$(4.6) \quad q_t + q_{xxx} = 0,$$

corresponding to $\omega(k) = -k^3$. Letting $s = y/t^{1/3}$ and $\lambda = kt^{1/3}$ one has, using similar methods as before,

$$(4.7) \quad I_{\text{stokes},0}(y, t) = \frac{1}{2\pi i} \int_C e^{i\lambda s - i\lambda^3} \frac{d\lambda}{\lambda} = \int_{s/\sqrt[3]{3}}^{\infty} \text{Ai}(z) dz,$$

where $\text{Ai}(z)$ is the classical Airy function (e.g., see [30, 33]), which admits the integral representation $\text{Ai}(z) = \int_{\mathbb{R}} e^{i\lambda z - i\lambda^3} d\lambda / (2\pi)$ [2]. The corresponding behavior is illustrated in Fig. 4.3.

Note that, since all the PDEs considered in this work are linear, the behavior arising from a negative jump is simply the reflection with respect to the horizontal axis of that for a positive jump. On the other hand, unlike the heat and Schrödinger equation, the Stokes equation does not possess left-right symmetry. So the values of $I_{\omega,0}(y, t)$ to the left

of the discontinuity are not symmetric to those to the right (as is evident from Fig. 4.3). Note also that the results for the Stokes equation with the opposite sign of dispersion (i.e., $q_t - q_{xxx} = 0$) are obtained by simply exchanging $x - c$ with $c - x$ (i.e., y with $-y$) in the above discussion.

Monomial dispersion relations and special functions. As we now show, all of the above results regarding the characterization of the behavior near a jump discontinuity are easily generalized to monomial dispersion relations.

Recall the definition (3.5) of $I_{\omega,0}(y, t)$, and let $\omega(k) = \omega_n k^n$. For simplicity, we take ω_n to be real-valued, so that the PDE is indeed dispersive, but in Section 7 we show that similar calculations are also easily carried out for dissipative PDEs. Performing the changes of variable

$$(4.8) \quad s = y/(|\omega_n|t)^{1/n}, \quad \lambda = (|\omega_n|t)^{1/n}k,$$

with some abuse of notation we have that $I_{\omega,0}(y, t) = I_{n,0}^\sigma(y, t)$ is given by

$$(4.9) \quad I_{n,0}^\sigma(y, t) = E_{n,1}^\sigma(s),$$

with $\sigma = \text{sign}(\omega_n)$, and where we have defined

$$(4.10) \quad E_{n,m}^\pm(s) = \frac{1}{2\pi} \int_C e^{i\lambda s \mp i\lambda^n} \frac{d\lambda}{(i\lambda)^m}.$$

Equation (4.9) clearly shows that, for all $n \in \mathbb{N}$, $I_{n,0}(y, t)$ is a similarity solution of the PDE (1.1). Moreover, we can write the generalization of (4.3) as:

$$(4.11) \quad \frac{d}{ds} E_{n,1}^\sigma(y, t) = E_{n,0}^\sigma(s),$$

where $E_n^\sigma(s) = E_{n,0}^\sigma(s)$ is given by

$$(4.12) \quad E_n^\pm(s) = \frac{1}{2\pi} \int_{\mathbb{R}} e^{i\lambda s \mp i\lambda^n} d\lambda.$$

Note that since there is no more singularity at $\lambda = 0$ in (4.12), the contour C was deformed back to the real axis. Note also that the two integrals are not independent, since

$$(4.13) \quad E_n^-(s) = -E_n^+(-s).$$

Integrating to get $I_{n,0}^\pm(y, t)$ [taking into account its limits as $y \rightarrow \pm\infty$ given by (3.7)] we then have

$$(4.14) \quad I_{n,0}^+(y, t) + I_{n,0}^-(-y, t) = -1,$$

which relates the behaviors of PDEs with positive and negative dispersion.

Now recall that $E_2^+(s) = e^{is^2/4 - i\pi/4}/(2\pi)$ and $E_3^+(s) = \text{Ai}(s/\sqrt[3]{3})/\sqrt[3]{3}$. Hence, the $E_n^\pm(s)$ [and with them $E_{n,m}^\pm(s)$ and $I_{n,m}^\pm(y, t)$] are generalizations of classical special functions. Thus, the analysis shows that, *for monomial dispersion relations, the leading-order behavior of the solution near a discontinuity is governed by a similarity solution expressed in terms of classical special functions.*

Center value and overshoot of the special functions. Recall that, while q_c contributes a constant offset to the solution, the value of $q(x, t)$ at $(c, 0)$ [as obtained from the reconstruction formula (3.6)] will differ from q_c , because, even though $q_{\text{res}}(0, 0) = 0$, in general, $\lim_{t \downarrow 0} I_{\omega,0}(0, t) \neq 0$.

For monomial dispersion relations, i.e., $\omega(k) = \omega_n k^n$, it is easy to see that $I_{n,0}(0, t)$ is actually independent of time. In fact, the value of $I_{n,0}(0, t)$ can be easily obtained explicitly. From (4.9) we have

$$I_{n,0}(0, t) = \frac{1}{2\pi} \oint_{\mathbb{R}} e^{\pm i\lambda^n} \frac{d\lambda}{i\lambda} - \frac{1}{2},$$

since $\text{Res}_{\lambda=0}[e^{\pm i\lambda^n}/(i\lambda)] = 1$. Now note that $\oint_{\mathbb{R}} e^{\pm i\lambda^n} d\lambda/(i\lambda) = 0$ for n even, while the same integral equals $\pm \int_{\mathbb{R}} \sin(\lambda^n) d\lambda/\lambda = \pm\pi/n$ for n odd. Hence we have simply

$$(4.15) \quad I_{n,0}(0, t) = \begin{cases} -\frac{1}{2}, & n \text{ even}, \\ -\frac{1}{2}(1 \pm 1/n), & n \text{ odd}. \end{cases}$$

One can carry out the analogy with the classical Gibbs phenomenon even further and compute the “overshoot” of these special functions — namely, the ratio of the maximum difference between the value of the special function and

n	max real	min real	max imag	min imag	max modulus
2	1.17025	-0.170246	0.243797	-0.243797	1.17066
3	1.27435	0	0	0	1.27435
4	1.11501	-0.115008	0.121603	-0.121603	1.10603
5	1.19824	-0.0159841	0	0	1.19824
6	1.10146	-0.101461	0.0819619	-0.0819619	1.10103
7	1.16611	-0.0308676	0	0	1.16611
8	1.0963	-0.0962954	0.0618324	-0.0618324	1.09625
9	1.14849	-0.0413221	0	0	1.14849
10	1.09384	-0.0938431	0.0496286	-0.0496286	1.09383
11	1.1374	-0.0487894	0	0	1.1374
60	1.08961	-0.0896059	0.0083311	-0.0083311	1.08961
120	1.08952	-0.0895187	0.00416638	-0.00416638	1.08952
180	1.0895	-0.0895026	0.00277769	-0.00277769	1.0895
240	1.0895	-0.089497	0.0020833	-0.0020833	1.0895
300	1.08949	-0.0894945	0.00166665	-0.00166665	1.08949

Table 1: Numerically computed values for the maximum and minimum of the real part, imaginary part and modulus of $G_n(y, t) = 1 + I_{n,0}(y, t)$ as a function of n . The overshoot converges to the Wilbraham-Gibbs constant g [cf. (4.16)].

the jump, compared to the jump size. Recall that the overshoot for the Gibbs phenomenon is given by the Wilbraham-Gibbs constant [20, 42] (see also [23]).

$$(4.16) \quad g = \frac{1}{\pi} \int_0^\pi \frac{\sin z}{z} dz - \frac{1}{2} \approx 0.089490 \dots$$

For example, the maximum value of the partial sum of the Fourier series for $\chi_{[-1,1]}(y)$ on $[-2, 2]$ will converge to $1 + g$, and its minimum to $-g$.

To examine the overshoot of the special functions, we look at $G_n(y, t) = I_{n,0}(y, t) + 1$, which converges pointwise to $\chi_{(0,\infty)}(y)$ for all $y \neq 0$ as $t \downarrow 0$. Specifically, we compute numerically the maximum and minimum of the real part, imaginary part and modulus of $G_n(y, t)$. Note that, for all $t \neq 0$, all such values are independent of t . Table 1 shows these values as a function of n . Surprisingly, the table shows that *these values converge to exactly the same constants as for the Gibbs phenomenon as $n \rightarrow \infty$!*

Indeed, a simple calculation shows why this is true. Integration by parts or a simple change of variable can be used to show that, as $n \rightarrow \infty$,

$$I_{n,0}(y, 1) = \frac{1}{2\pi i} \int_{C'} e^{iky - ik^n} \frac{dk}{k} + O(1/n),$$

where $C' = C \cap \{k \in \mathbb{C} : |\operatorname{Re} k| \leq 1\}$, and where without loss of generality the semi-circle component of C was taken to have radius less than one. Then, by the dominated convergence theorem we have

$$\lim_{n \rightarrow \infty} \frac{1}{2\pi i} \int_{C'} e^{iky - ik^n} \frac{dk}{k} = \frac{1}{2\pi i} \int_{C'} e^{iky} \frac{dk}{k},$$

where convergence is uniform in y . Moreover, the integral on the RHS is easily shown to be

$$\frac{1}{2\pi i} \int_{C'} e^{iky} \frac{dk}{k} = \frac{1}{2\pi} \int_{-1}^1 \frac{\sin ky}{k} dk - \frac{1}{2},$$

where the contour in the RHS was deformed back to the real axis since there is a removable singularity at $k = 0$. After a simple rescaling we then have

$$(4.17) \quad \lim_{n \rightarrow \infty} I_{n,0}(y, 1) = \frac{1}{\pi} \int_0^\pi \frac{\sin(\pi y z)}{z} dz - \frac{1}{2},$$

uniformly in y . This integral is maximized and minimized at $y = \pm 1$, respectively, yielding

$$\begin{aligned} \lim_{n \rightarrow \infty} \sup_{y \in \mathbb{R}} \operatorname{Re} G_n(y, 1) &= 1 + g, & \lim_{n \rightarrow \infty} \sup_{y \in \mathbb{R}} \operatorname{Im} G_n(y, 1) &= 0, \\ \lim_{n \rightarrow \infty} \inf_{y \in \mathbb{R}} \operatorname{Re} G_n(y, 1) &= -g, & \lim_{n \rightarrow \infty} \inf_{y \in \mathbb{R}} \operatorname{Im} G_n(y, 1) &= 0. \end{aligned}$$

Note that for a fixed value of n such maxima and minima can occur on either side of the jump (e.g., cf. Figs. 4.2 and 4.3).

Another way to summarize this behavior is to use two theorems. The first is a restatement of the results of Wilbraham and Gibbs ([42] and [20]):

Theorem 4.1. *Consider the Fourier series approximation of*

$$f(x) = \begin{cases} 1, & \text{if } |x| \leq 1, \\ 0, & \text{otherwise,} \end{cases} \quad \text{given by } S_n[f](x) = \sum_{k=-n}^n \frac{4 \sin \frac{k\pi}{2}}{k\pi} e^{\frac{ikx\pi}{2}}.$$

Then for any $\delta > 0$

$$\begin{aligned} \lim_{n \rightarrow \infty} \sup_{|x \pm 1| \leq \delta} S_n[f](x) &= 1 + g, \\ \lim_{n \rightarrow \infty} \inf_{|x \pm 1| \leq \delta} S_n[f](x) &= -g. \end{aligned}$$

In this context our results give:

Theorem 4.2. *Let $q_n(x, t)$ be the solution of $iq_t - (-i\partial_x)^n q = 0$ with*

$$q(x, 0) = \begin{cases} 1, & \text{if } |x| \leq 1, \\ 0, & \text{otherwise.} \end{cases}$$

Then for any $\delta > 0$

$$\begin{aligned} \lim_{n \rightarrow \infty} \lim_{t \downarrow 0} \sup_{|x \pm 1| \leq \delta} \operatorname{Re} q_n(x, t) &= 1 + g, \\ \lim_{n \rightarrow \infty} \lim_{t \downarrow 0} \inf_{|x \pm 1| \leq \delta} \operatorname{Re} q_n(x, t) &= -g, \\ \lim_{n \rightarrow \infty} \lim_{t \downarrow 0} \sup_{|x \pm 1| \leq \delta} \operatorname{Im} q_n(x, t) &= 0, \\ \lim_{n \rightarrow \infty} \lim_{t \downarrow 0} \inf_{|x \pm 1| \leq \delta} \operatorname{Im} q_n(x, t) &= 0. \end{aligned}$$

Remark 4.1. *One does not have to take $\omega(k) = k^n$ in the previous theorem: It follows for general $\omega(k)$ provided the coefficients are appropriately controlled. One such example is $\omega(k) = k^n + \sum_{j=n-m}^{n-1} c_{j,n} k^j$ where $|c_{j,n}| \leq C$ and m is fixed.*

5. Short-time asymptotics: ICs with discontinuous derivatives

We now treat the case where one of the derivatives of q_o is discontinuous. We begin by assuming a discontinuity in the first derivative, then we treat the general case. We will further generalize the results in section 6.

Assumption 5.1. *Let*

- $q_o \in H^1(\mathbb{R})$,
- $[q'_o(c)] = q'_o(c^+) - q'_o(c^-) \neq 0$,
- q''_o exists on $(-\infty, c) \cup (c, \infty)$,
- $q''_o \in L^q(-\infty, c) \cap L^q(c, \infty)$ for some $1 < q < \infty$, and
- q_o is compactly supported.

Assuming compact support avoids possible complications arising from the non-existence of some principal value integrals. (This assumption will be removed in section 6.) We will show that the asymptotic behavior in the regularization region is given by integrals of the special functions considered in the previous section.

Note first that, if $F(k)$ is analytic in a neighborhood of the origin, (3.3) can be written as

$$q(x, t) = [q_o(c)]I_{\omega,0}(x - c, t) + \frac{1}{2\pi} \int_C e^{i\theta(x,t,k)} F(k) \frac{dk}{ik},$$

with $I_{\omega,0}(y, t)$ and $F(k)$ given by (3.5) and (3.2), respectively, and with C as in Figure 3.1. Analyticity of F is always guaranteed if q_o has compact support. In the case that q_o is continuous but q'_o is discontinuous, we perform one more

integration by parts and write

$$(5.1) \quad q(x, t) = [q'_o(c)]I_{\omega,1}(x - c, t) + \frac{1}{2\pi} \int_c^\infty e^{i\theta(x,t,k)} F_1(k) \frac{dk}{(ik)^2},$$

where

$$F_1(k) = \left(\int_{-\infty}^c + \int_c^\infty \right) e^{-iks} q''_o(s) ds,$$

and where we have introduced the generalization of $I_{\omega,0}(y, t)$ as

$$(5.2) \quad I_{\omega,m}(y, t) = \frac{1}{2\pi} \int_c^\infty \frac{e^{iky - i\omega(k)t}}{(ik)^{m+1}} dk.$$

As before, we now expand (5.1) both near and away from the singularity c . In a neighborhood of $(c, 0)$, we leave $I_{\omega,1}(y, t)$ alone, and we expand $F_1(k)$. As $k \rightarrow 0$,

$$e^{ikc} e^{i\theta(x-c,t,k)} = e^{ikc} (1 + ik(x - c) + O(k^2)).$$

We then have

$$q(x, t) = [q'_o(c)]I_{\omega,1}(x - c, t) + \frac{1}{2\pi} \int_c^\infty e^{ikc} \left(\frac{1 + ik(x - c)}{(ik)^2} \right) F_1(k) dk + q_{\text{res},1}(x - c, t),$$

where

$$q_{\text{res},1}(x - c, t) = \frac{1}{2\pi} \int_{\mathbb{R}} e^{ikc} \left(\frac{e^{i\theta(x-c,t,k)} - 1 - ik(x - c)}{(ik)^2} \right) F_1(k) dk.$$

We expect $q_{\text{res},1}(y, t)$ to give a lower order contribution as $(x, t) \rightarrow (c, 0)$. We thus examine this expression in the regularization region $|x - c| \leq Ct^n$. Lemma C.1 indicates that $q_{\text{res},1}(x, t) = O(t^{1/n+1/(np)})$ because $F \in L^p(\mathbb{R})$ (where $1/p + 1/q = 1$). Therefore $q_{\text{res},1}(y, t)$ can indeed be seen as the error term.

We now examine (5.1) for $|x - c| \geq \delta > 0$ and $|s - x| \leq \delta/2$. We have

$$\begin{aligned} q(x, t) - q_o(s) &= [q'_o(c)](I_{\omega,1}(x - c, t) - I_{\omega,1}(s - c, 0)) + \frac{1}{2\pi} \int_c^\infty e^{iks} (e^{i\theta(x-s,t,k)} - 1) F_1(k) \frac{dk}{(ik)^2} \\ &= [q'_o(c)](I_{\omega,1}(x - c, t) - I_{\omega,1}(s - c, 0)) + \frac{(x - s)}{2\pi} \int_c^\infty e^{iks} F_1(k) \frac{dk}{ik} + q_{\text{res},1}(x - s, t). \end{aligned}$$

Applying Theorem B.6 and Lemma C.1, in the regularization region $|x - s|^n \leq Ct$ we have

$$\begin{aligned} q(x, t) &= q_o(s) + [q'_o(c)]((s - c)\chi_{(-\infty, c)}(s) - (x - c)\chi_{(-\infty, c)}(x)) \\ &\quad + \frac{(x - s)}{2\pi} \int_c^\infty e^{iks} F_1(k) \frac{dk}{ik} + O\left(t^{3/(2(n-1))} + t^{1/n+1/(np)}\right). \end{aligned}$$

This expression is simplified using $\chi_{(-\infty, c)}(s) = \chi_{(-\infty, c)}(x)$ and the relation

$$\frac{(x - s)}{2\pi} \int_c^\infty e^{iks} F_1(k) \frac{dk}{ik} = -\frac{1}{2} [q'_o(c)](x - s) + \frac{(x - s)}{2\pi} \oint_c^\infty e^{iks} F_1(k) \frac{dk}{ik},$$

to obtain

$$\begin{aligned} q(x, t) &= q_o(s) + [q'_o(c)](s - x)(-1/2 + \chi_{(-\infty, c)}(s)) \\ &\quad + \frac{(x - s)}{2\pi} \oint_c^\infty e^{iks} F_1(k) \frac{dk}{ik} + O\left(t^{3/(2(n-1))} + t^{1/n+1/(np)}\right). \end{aligned}$$

Next we generalize the above result to a discontinuity in a derivative of arbitrary order:

Assumption 5.2. *Let*

- $q_o \in H^m(\mathbb{R})$,
- $[q_o^{(m)}(c)] \neq 0$,
- $q_o^{(m+1)}$ exists on $(-\infty, c) \cup (c, \infty)$, separately,
- $q_o^{(m+1)} \in L^q(-\infty, c) \cap L^q(c, \infty)$ for some $1 < q < \infty$, and
- q_o is compactly supported.

Let $a_\ell(y, t)$ be the Taylor coefficients of $e^{i\theta(y, t, k)}$ at $k = 0$. Then for $s \in \mathbb{R}$ (possibly equal to c) we find the expansion

$$(5.3) \quad q(x, t) = [q_o^{(m)}(c)]I_{\omega, m}(x - c, t) + \frac{1}{2\pi} \int_C e^{iks} \left(\sum_{\ell=0}^m a_\ell(x - s, t) k^\ell \right) F_m(k) \frac{dk}{(ik)^{m+1}} + q_{\text{res}, m}(x - s, t),$$

where

$$q_{\text{res}, m}(x - s, t) = \frac{1}{2\pi} \int_{\mathbb{R}} e^{iks} \left(e^{i\theta(x-s, t, k)} - \sum_{\ell=0}^m a_\ell(x - s, t) k^\ell \right) F_m(k) \frac{dk}{(ik)^{m+1}},$$

$$F_m(k) = \left(\int_{-\infty}^c + \int_c^\infty \right) e^{-ikx} q_o^{(m+1)}(x) dx.$$

Invoking Lemma C.1, this expression provides the asymptotic expansion in the regularization region $|x - s|^n \leq Ct$. Indeed, $q_{\text{res}, m}(x, t) = O(t^{m/n+1/(pn)})$ for $1/p + 1/q = 1$. This expansion can be understood more thoroughly as follows. Formally, for $s \in \mathbb{R}$

$$(5.4) \quad (-i\partial_x)^j q_o(s) = [q_o^{(m)}(c)] \text{Res}_{k=0} \left(\frac{e^{ik(s-c)}}{i(ik)^{m-j+1}} \right) \chi_{(-\infty, 0)}(s - c) + \frac{1}{2\pi} \int_C e^{iks} F_m(k) \frac{dk}{(ik)^{m-j+1}}.$$

We next show that

$$(5.5) \quad \sum_{j=0}^M \frac{(-it)^j}{j!} \omega(-i\partial_x)^j = \sum_{\ell=0}^{nM} a_\ell(0, t) k^\ell + O(t^{M+1} k^{nM}),$$

as $|k| \rightarrow \infty$ and $t \downarrow 0$. To see this, it follows from Lemma C.1 that $a_\ell(0, t) = O(t^{\ell/n})$ and then

$$e^{-i\omega(k)t} - \sum_{\ell=0}^{nM} a_\ell(0, t) k^\ell = O(t^{M+1})$$

as $t \downarrow 0$, because only integer powers of t appear. Then

$$e^{-i\omega(k)t} - \sum_{j=0}^M \frac{(-it)^j}{j!} \omega(-i\partial_x)^j = O(t^{M+1}),$$

implying

$$\sum_{j=0}^M \frac{(-it)^j}{j!} \omega(-i\partial_x)^j = \sum_{\ell=0}^{nM} a_\ell(0, t) k^\ell + O(t^{M+1}).$$

Then (5.5) follows by noting that both sides have no powers of k larger than k^{nM} . In turn, (5.5) implies

$$(5.6) \quad \sum_{j=0}^M \frac{(-it)^j}{j!} \omega(-i\partial_x)^j q_o(s) = [q_o^{(m)}(c)] \text{Res}_{k=0} \left(\frac{e^{ik(s-c)}}{i(ik)^{m+1}} \sum_{\ell=0}^{nM} a_\ell(0, t) k^\ell \right) \chi_{(-\infty, 0)}(s - c)$$

$$(5.7) \quad + \frac{1}{2\pi} \int_C e^{iks} \left(\sum_{\ell=0}^{nM} a_\ell(0, t) k^\ell \right) F_m(k) \frac{dk}{(ik)^{m+1}} + O(t^{M+1}).$$

If $s \neq c$ then this expression is well-defined and continuous for $nM \leq m$. If $s = c$, there are issues concerning the definition of the value of $q_o^{(nM)}(c)$ on the left-hand side of the equation and we must restrict to $nM < m$.

Near the singularity. Let $M = \lfloor (m-1)/n \rfloor$. For $|x - c|^n \leq Ct$ we combine (5.6) and (5.3) to find

$$(5.8) \quad q(x, t) = \sum_{j=0}^M \frac{(-it)^j}{j!} \omega(-i\partial_x)^j q_o(c) + [q_o^{(m)}(c)]I_{\omega, m}(x - c, t) + \frac{1}{2\pi} \int_C e^{ikc} \left(\sum_{\ell=0}^m (a_\ell(x - c, t) - a_\ell(0, t)) k^\ell \right) F_m(k) \frac{dk}{(ik)^{m+1}} + O\left(t^{\frac{m}{n} + \frac{1}{np}}\right).$$

Here, the residue term in (5.4) vanishes at $s = c$ because $Mn < m$ and no k^{-1} term is present. It also follows (see Lemma C.1) that $a_\ell(x - c, t) = O(t^{\ell/n})$ so that this is indeed a consistent expansion.

Away from the singularity. Let $M = \lfloor m/n \rfloor$. We examine the expansion for near $x = s$ for $|s - c| \geq \delta > 0$. We use the short-time asymptotics for $I_{\omega,m}$ (see Theorem B.6) to find for $|x - s|^n \leq C|t|$

$$(5.9) \quad \begin{aligned} q(x, t) &= \sum_{j=0}^M \frac{(-it)^j}{j!} \omega(-i\partial_x)^j q_o(s) \\ &+ \frac{1}{2\pi} \int_C e^{iks} \left(\sum_{\ell=0}^m (a_\ell(x-s, t) - a_\ell(0, t)) k^\ell \right) F_m(k) \frac{dk}{(ik)^{m+1}} \\ &- i[q_o^{(m)}(c)] \operatorname{Res}_{k=0} \left(\frac{e^{ik(x-c)-i\omega(k)t}}{(ik)^{m+1}} - \frac{e^{ik(s-c)}}{(ik)^{m+1}} \sum_{j=0}^M \frac{(-i\omega(k)t)^j}{j!} \right) \chi_{(-\infty, 0)}(s-c) \\ &+ O\left(t^{\frac{m}{n}} \left(t^{\frac{1}{np}} + t^{\frac{n+2m}{2n(n-1)}} \right)\right). \end{aligned}$$

If we set $x = s$ then the residue term is $O(t^{M+1})$ ($m/n + 1/n \leq M + 1$) and the short-time Taylor expansion

$$(5.10) \quad q(x, t) = \sum_{j=0}^M \frac{(-it)^j}{j!} \omega(-i\partial_x)^j q_0(x) + O\left(t^{\frac{m}{n}} \left(t^{\frac{1}{np}} + t^{\frac{n+2m}{2n(n-1)}} \right)\right).$$

follows. Here the error term is uniform in x as x varies in the region $|x - c| \geq \delta$. Thus, in particular, if q_o vanishes identically in a neighborhood of s then for $|x - s|^n \leq C|t|$

$$(5.11) \quad q(x, t) = O\left(t^{\frac{m}{n}} \left(t^{\frac{1}{np}} + t^{\frac{n+2m}{2n(n-1)}} \right)\right).$$

A unified formula. We now introduce some convenient and unifying notation that will be useful to combine the above results. Define

$$\begin{aligned} R_{M,m,c}(q_o; x, s) &= -i[q_o^{(m)}(c)] \operatorname{Res}_{k=0} \left(\frac{e^{ik(x-c)-i\omega(k)t}}{(ik)^{m+1}} - \frac{e^{ik(s-c)}}{(ik)^{m+1}} \sum_{j=0}^M \frac{(-i\omega(k)t)^j}{j!} \right) \chi_{(-\infty, 0)}(s-c), \\ A_m(q_o; x, s) &= \frac{1}{2\pi} \int_C e^{iks} \left(\sum_{\ell=0}^m (a_\ell(x-s, t) - a_\ell(0, t)) k^\ell \right) F_m(k) \frac{dk}{(ik)^{m+1}}. \end{aligned}$$

Note $A_m(q; x, s)$ can only be applied to functions whose Fourier transform is analytic in a neighborhood of the origin. Therefore we have for $M = 0, \dots, \lfloor \frac{m-1}{n} \rfloor$ and $s \in \mathbb{R}$,

$$q(x, t) = \sum_{j=0}^M \frac{(-it)^j}{j!} \omega(-i\partial_x)^j q_o(s) + A_m(q_o; x, s) + \begin{cases} R_{M,m,c}(q_o; x, s), & s \neq c, \\ [q_o^{(m)}(c)] I_{\omega,m}(x-c, t), & s = c, \end{cases} + O\left(t^{\frac{m}{n}} \left(t^{\frac{1}{np}} + t^{\frac{n+2m}{2n(n-1)}} \right)\right).$$

While the formula for $s \neq c$ is also valid for $M = \lfloor m/n \rfloor$, this is a convenient form. Furthermore, when no singularity is present locally, (5.10) provides a cleaner formula in terms of quantities that are easier to compute. We note that A_m and $R_{M,m,c}$ ($s \neq c$) contain terms that are analytic in x and t while $I_{\omega,m}$ encodes the dominant behavior near the singularity; *i.e.*, it has a discontinuous derivative at some order.

6. Short-time asymptotics: ICs with multiple singular points and non-compact support

We now discuss the case of ICs with multiple points of discontinuity. The results in this section are the most general ones of this work regarding the short-time behavior of the solution of dispersive PDEs.

Assumption 6.1. For $c_0 = -\infty < c_1 < \dots < c_N < c_{N+1} = +\infty$, let

- $q_o \in H^m(\mathbb{R}) \cap L^1((1+|x|)^\ell dx)$, with $\ell \geq \mathfrak{C}_n$,
- $[q_o^{(m)}(c_i)] \neq 0$ for $i = 1, \dots, N$,
- $q_o^{(m+1)}(x)$ exists on (c_{i-1}, c_i) for $i = 1, \dots, N+1$,
- $q_o^{(m+1)} \in L^2(c_{i-1}, c_i)$ for $i = 1, \dots, N+1$.

Note that we have removed the assumption of compact support. The key to do so is to use a Van der Corput *neutralizer* (or “bump” function) (e.g., see [2]), namely a function that interpolates infinitely smoothly between 0 and 1. More precisely, for our purposes a neutralizer is a function $\eta_\delta(y)$ with the following properties:

- it possesses continuous derivatives of all orders;
- $\eta_\delta(y) = 1$ for $y < \delta/2$ and $\eta_\delta(y) = 0$ for $y > \delta$;

(iii) the derivatives of $\eta_\delta(y)$ of all orders vanish at $y = \delta/2$ and $y = \delta$.

A suitable definition is given by

$$\eta_\delta(y) = n(\delta - x)/[n(y - \delta/2) + n(\delta - x)]$$

where

$$n(y) = \begin{cases} 1, & y < 0, \\ e^{-1/y}, & y > 0, \end{cases}$$

but the actual form of the neutralizer is irrelevant for what follows. Then, to study the behavior near each discontinuity $(x, t) = (c_j, 0)$, for $j = 1, \dots, N$, one can decompose the IC as

$$(6.1) \quad q_o(x) = \sum_{j=1}^m q_{o,j}(x) + q_{o,\text{reg}}(x),$$

where

$$(6.2) \quad q_{o,j}(x) = q_o(x) \eta_\delta(|x - c_j|),$$

and

$$(6.3) \quad q_{o,\text{reg}}(x) = q_o(x) \left(1 - \sum_{j=1}^m \eta_\delta(|x - c_j|)\right),$$

with $\delta < \min_{j=1, \dots, m-1} (c_{j+1} - c_j)/2$. Correspondingly, the solution of the PDE is decomposed as

$$(6.4) \quad q(x, t) = \sum_{j=1}^m q_j(x, t) + q_{\text{reg}}(x, t).$$

Note that each $q_{o,j}^{(m)}(x)$ is discontinuous but compactly supported, while $q_{o,\text{reg}}^{(m)}(x)$ is non-compactly supported but continuous. Moreover, $q_{o,j}(c_{j'}) = 0$ for all $j' \neq j$, and $q_{o,\text{reg}}(c_j) = 0$ for $j = 1, \dots, m$. Importantly, it follows that $q_{o,\text{reg}} \in H^{m+1}(\mathbb{R})$. Noting that $[q_{o,\text{reg}}^{(m)}(c)] = 0$, with $nM \leq m < n(M+1)$, by (5.10) we have

$$q_{\text{reg}}(x, t) = \sum_{j=0}^M \frac{(-it)^j}{j!} \omega(-i\partial_x)^j q_{o,\text{reg}}(x) + O(t^{m/n+1/(2n)}).$$

In the regularization region $|x - c_j|^n \leq Ct$, all derivatives of $q_{o,\text{reg}}$ vanish identically so that $q_{\text{reg}}(x, t) = O(t^{m/n+1/(2n)}) = q_{j'}(x, t)$ for $j' \neq j$, see (5.11).

We state our main asymptotic result as a theorem.

Theorem 6.1. *Suppose Assumption 6.1 holds, and let $\mathcal{D} = \{c_j\}_{j=1}^N$.*

- *If $|x - c_j|^n \leq C|t|$ then for $M = \lfloor \frac{m-1}{n} \rfloor$*

$$(6.5) \quad \begin{aligned} q(x, t) = & \sum_{j=0}^M \frac{(-it)^j}{j!} \omega(-i\partial_x)^j q_o(c_j) + [q_o^{(m)}(c_j)] I_{\omega,m}(x - c_j, t) \\ & + A_m(q_{o,j}; x, c_j) + O\left(t^{\frac{m}{n}} \left(t^{\frac{1}{2n}} + t^{\frac{n+2m}{2n(n-1)}}\right)\right). \end{aligned}$$

- *If $|c_j - x| \geq \delta > 0$ for all j then for $M = \lfloor \frac{m}{n} \rfloor$*

$$q(x, t) = \sum_{j=0}^M \frac{(-it)^j}{j!} \omega(-i\partial_x)^j q_o(x) + O\left(t^{\frac{m}{n}} \left(t^{\frac{1}{2n}} + t^{\frac{n+2m}{2n(n-1)}}\right)\right).$$

Proof. We use linearity. As discussed, we apply (5.10) and (5.11) so that $q_{\text{reg}}(x, t) = O(t^{m/n+1/(2n)})$. The first claim follows from (5.8) and (5.9). The final claim follows from (5.10). \square

From (6.5) we conclude that near a singularity $q(x, t)$ can be written as $I_{\omega,m}$ plus lower-order and analytic terms. We not only have an asymptotic expansion but an expansion that separates regularity properly. Furthermore, the expansion about c_j depends only on local properties of q_o through $q_{o,j}$.

7. Further analysis and computation of the special functions

It should be abundantly clear from sections 3–6 that the integrals $I_{\omega,n}(y, t)$ [defined in (5.2)] play a crucial role in the analysis. The detailed properties of these integrals are discussed in Appendix B. Here we mention some further properties of these objects and we outline an efficient computational approach for their numerical evaluation.

Monomial dispersion relations. Like their simpler counterparts $I_{\omega,0}(y, t)$, the integrals $I_{\omega,n}(y, t)$ take on a particularly simple form in the case of a monomial dispersion relation, namely, $\omega(k) = \omega_n k^n$. Taking again $\omega_n \in \mathbb{R}$, we have

$$(7.1) \quad I_{n,m}(y, t) = (|\omega_n|t)^{m/n} E_{n,m}^\sigma(s),$$

where $s = y/(|\omega_n|t)^{1/n}$ and $\sigma = \text{sign}(\omega_n)$ as before, and now

$$(7.2) \quad E_{n,m}^\mp(s) = \frac{1}{2\pi} \int_C e^{i\lambda s \mp i\lambda^n} \frac{d\lambda}{(i\lambda)^{m+1}}.$$

We then have a generalization of (4.11):

$$(7.3) \quad \frac{d}{ds} E_{n,m}^\sigma(s) = E_{n,m-1}^\sigma(s).$$

So in principle one could obtain $E_{n,m}^\sigma(s)$ by integrating the right-hand side of (7.3) and by fixing the integration constant appropriately. In practice, however, it is more convenient to evaluate the integral for $E_{n,m}^\sigma(s)$ directly, using the methods discussed below.

General dispersion relations. Following arguments from Lemma B.4, for $t > 0$, $I_{\omega,m}(y, t)$ may be deformed to a contour that is asymptotically on the path of steepest descent for $e^{-i\omega(k)t}$. Let C be this contour. From this deformation, differentiability follows and

$$(7.4) \quad \partial_y^j I_{\omega,m}(y, t) = I_{\omega,m-j}(y, t).$$

Yet more structure is present. A straightforward calculation using integration by parts shows

$$-it\omega'(-i\partial_y)I_{\omega,m}(y, t) = \frac{1}{\pi} \int_C -it\omega'(k) \frac{e^{iky-i\omega(k)t}}{(ik)^{m+1}} dk = yI_{\omega,m}(y, t).$$

We thus have obtained the $(n-1)^{\text{th}}$ -order differential equation

$$(7.5) \quad \omega'(-i\partial_y)I_{\omega,m}(y, t) = \frac{iy}{t} I_{\omega,m}(y, t),$$

satisfied by $I_{\omega,m}(y, t)$.

Dissipative PDEs. The results in section 4 are easily modified when ω_n is not real, i.e., when one is dealing with a dissipative PDE. Recall that, for well-posedness, this can only happen when n is even, in which case $\omega_n = -i|\omega_n|$. In this case one can still perform the changes of variables (4.8), but the result is now

$$(7.6) \quad I_{n,0}(y, t) = E_{n,1}^o(s(y)),$$

where

$$(7.7) \quad E_{n,m}^o(s) \triangleq \frac{1}{2\pi} \int_C e^{i\lambda s - \lambda^n} \frac{d\lambda}{(i\lambda)^m}.$$

Equation (4.11) also remains valid, but now

$$(7.8) \quad E_n^o(s) \triangleq \frac{1}{2\pi} \int_{\mathbb{R}} e^{i\lambda s - \lambda^n} d\lambda.$$

An alternative approach is to perform a complex rescaling, by defining $s = y/(\omega_n t)^{1/n}$ and $\lambda = (\omega_n t)^{1/n} k$. The rescaling that is performed to express $I_{n,0}(y, t)$ in terms of $E_{n,1}(s)$ actually changes the integration contour in the complex plane from C into a rotated contour \tilde{C} . On the other hand, the same conditions on ω_n that ensure well-posedness guarantee that the integrand vanishes exponentially fast along a circular arc of radius R that connects C to \tilde{C} as $R \rightarrow \infty$. Thus, one can always rotate \tilde{C} back to C . As a result, when ω_n is not real, one obtains the special functions $E_{n,1}^+(s)$ evaluated at complex arguments (e.g., compare the situation for the heat equation and the Schrödinger equation). But, again, the same conditions on ω_n that ensure well-posedness guarantee the convergence of the integral in (4.9) and (4.12). The two approaches of course are equivalent.

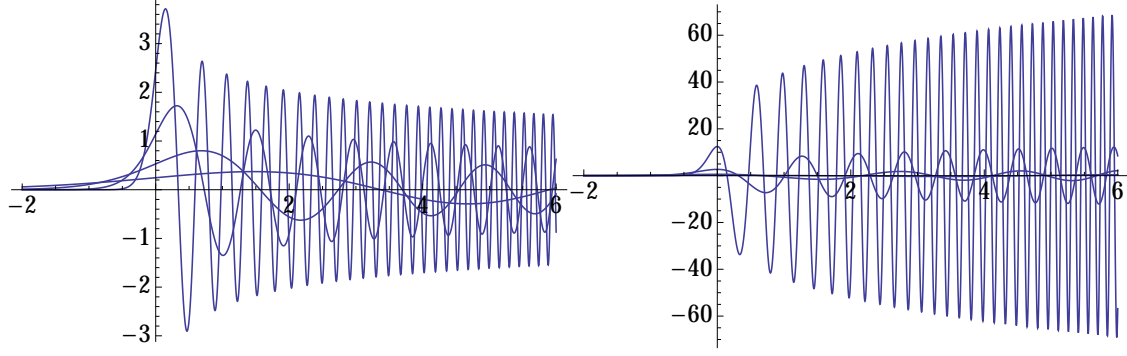


Figure 7.1: Plots of $I_{\omega,m}(y, t)$ with $\omega(k) = k^3$ versus y for $t = 1, 0.1, 0.01, 0.001$. Left: The scaled Airy function ($m = 0$). Right: The first derivative of the scaled Airy function ($m = 1$).

Numerical computation of the special functions. Next, we discuss the numerical evaluation of $I_{\omega,m}(y, t)$ for all y and t . First, introduce $\omega_t(k) = \omega(kt^{-1/n})t = \omega_n k^n + O(t^{1/n}k^{n-1})$. Then

$$I_{\omega,m}(y, t) = t^{(m-1)/n} I_{\omega_t,m}(yt^{-1/n}, 1).$$

It is important that $\omega_t(k) \approx \omega_n k^n$ for t small. We consider the computation of $I_{\omega_t,m}(s, 1)$ accurately for all $s \in \mathbb{R}$. The numerical method for accomplishing this follows the proof of Theorem B.6. Specifically, we use quadrature along the contours Γ_j . Since the precise paths of steepest descent do not need to be followed, we use piecewise-affine contours such that the angle of the contour that passes through each κ_j agrees with the local path of steepest descent. The routines in [34] provide a robust framework for visualizing and computing such contour integrals. In general, Clenshaw–Curtis quadrature is used on each affine component. To ensure accuracy for arbitrarily large s , the contour that passes through κ_j is chosen to be of length proportional to $1/\sqrt{|s\omega_t''(\kappa_j)|}$. This ensures that the Gaussian behavior near the stationary point is captured accurately in the large s limit. If all deformations are performed correctly, with this scaling behavior, a fixed number of sample points for Clenshaw–Curtis can be used for all x . A more in-depth discussion of this idea is given in [38].

For reference purposes, the above method should be compared to a more restricted approach for the computation of generalized Airy functions presented in [6].

Example 1: Airy function. When $\omega(k) = k^3$, the functions $I_{\omega,m}(y, t)$ are scaled derivatives and primitives of the Airy function. This function is displayed in Figure 7.1 for various values of t . See also Fig. 4.3, where a primitive of the scaled Airy function ($m = -1$) was shown. [But note that in Fig. 4.3 the dispersion relation was $\omega(k) = -k^3$, which results in a switch $y \mapsto -y$.] It is clear that while the Airy function is bounded, its derivative grows in x . This is in agreement with Theorem B.6.

Example 2: A higher-order solution. When the dispersion relation is non-monomial, the situation is more complicated. Consider for example $\omega(k) = k^4 + 2k^3$. In this case $I_{\omega,m}(y, t)$ is no longer a similarity solution. Furthermore, it has non-zero real and imaginary parts. This function is displayed in Figure 7.2 for various values of t .

8. Concluding remarks

We have obtained an asymptotic expansion for the short-time asymptotics of the solution of linear evolution PDEs with discontinuous ICs, including precise error estimates. The results apply to generic ICs (i.e., non-piecewise constant, non-compact support). Moreover, the results extend to arbitrary dispersion relations, multiple discontinuities, and discontinuous derivatives of the IC. In a forthcoming publication we will show that these results are also instrumental to characterize discontinuous BCs and corner singularities in IBVPs using the unified approach presented in [19]. We end this work with a further discussion of the results.

1. We have shown that the short-time asymptotic behavior of the solution of an evolution PDE with singular ICs is governed by similarity solutions and classical special functions. This is analogous to what happens in the long-time asymptotic behavior. In that case, however, it is the discontinuities of the Fourier transform that provide the singular points for the analysis (in addition of course to the stationary points or saddle points characteristic of the PDE). In

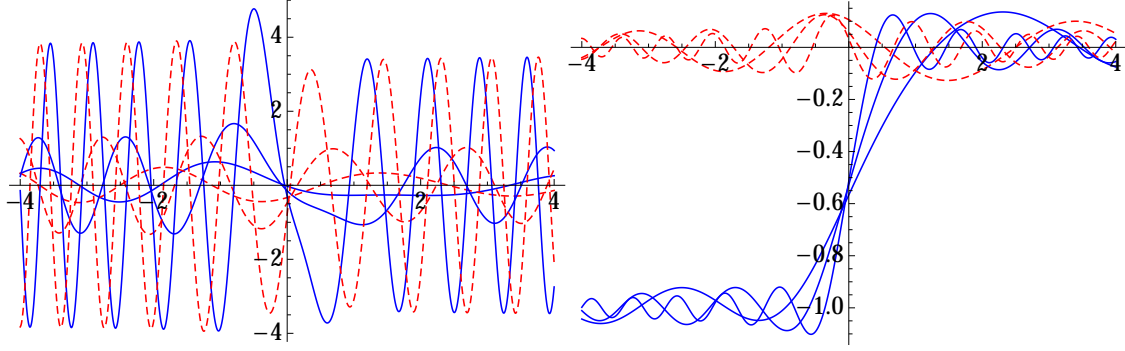


Figure 7.2: Plots of $I_{\omega,m}(y,t)$ with $\omega(k) = k^4 + 2k^3$ versus y for $t = 0.1, 0.01, 0.001$ (solid: real part, dashed: imaginary part). Left: $m = 1$. Right: $m = -1$.

turn, these are related to the slow decay of the ICs at infinity. In this sense, the short-time and long-time behavior are dual expressions of the characteristic behavior of a linear PDE.

2. We have also shown that the solutions of dispersive linear PDEs exhibits Gibbs-like behavior in the short-time limit. This Gibbs-like behavior is robust, meaning that it persists under perturbation. To explain this point, one should consider the obvious question of what happens with ICs which are a “smoothed out” discontinuity, namely, a sharp but continuous transition from one value to a different one. Such an IC can be considered to be a small perturbation of a step discontinuity in $L^2(\mathbb{R}) \cap L^1((1+|x|)^\ell)$. Thus, as long as the IVP is well-posed, the continuous dependence of the solution of the IVP on the ICs implies that a small change in the ICs will only produce a small change in the solution.

Let us briefly elaborate on this point. Obviously if the perturbed IC is continuous, the solution of the PDE will converge uniformly to it as $t \downarrow 0$. Therefore, the Gibbs phenomenon that is present for the unperturbed solution will eventually disappear in the perturbed solution in this limit. On the other hand, in Appendix D we show that, if the perturbation is sufficiently small, one can still expect to observe a similar Gibbs-like effect *at finite times*.

3. The Gibbs-like behavior has been noticed in a couple of cases for nonlinear PDEs. In particular, DiFranco and McLaughlin [10] studied the behavior of the defocusing nonlinear Schrödinger (NLS) equation with box-type IC, while Kotlyarov and Minakov [29] studied the behavior of the Korteweg-de Vries (KdV) and modified KdV equations with Heaviside ICs. In both cases, these authors showed that the behavior of the nonlinear PDE for short times is given to leading order by the behavior of the linear PDE. And in both cases, in order to characterize the phenomenon it was necessary to use complete integrability of the nonlinear PDEs, as well as Deift and Zhou’s nonlinear analogue of the steepest descent method for oscillatory Riemann-Hilbert problems [8, 9]. But the results of this work make it clear that this behavior: (i) is not a nonlinear phenomenon, and it also applies to linear PDEs; (ii) is a general phenomenon, not limited to a few special PDEs.

4. At the same time it is true that for many nonlinear PDEs the nonlinear terms require $O(1)$ times in order to produce an appreciable effect on the solution. Therefore it is reasonable to expect that the results of this work will also provide the leading-order behavior of the solution of many nonlinear PDEs for short times. Indeed, Taylor [39] studied a generalized NLS equation (which is not completely integrable), and again characterized the behavior of the solutions for short times in terms of those of the linearized PDE. It is hoped that such results can be generalized to other kinds of nonlinear PDEs.

5. Of course, for larger times the solutions of linear and nonlinear PDEs with discontinuous ICs are very different from each other: While for linear PDEs the oscillations spread out thanks to the similarity variable, for nonlinear PDEs the discontinuity gives rise to dispersive shock waves (DSWs); namely, an expanding train of modulated elliptic oscillations with a fixed spatial period, whose envelope interpolates between the values of the solution at either side of the jump. Such a nonlinear phenomenon has been known since the 1960’s [22], and a large body of work has been devoted to its study (e.g., see [3, 11, 12, 13, 21, 24, 25, 26, 28] and references therein). To the best of our knowledge, however, such behavior was never compared to the corresponding one for linear PDEs, unlike what was done for the long-time asymptotics (e.g., see [1, 32]).

6. We reiterate that this Gibbs-like behavior of dispersive PDEs *is not a numerical artifact of a numerical approximation to the solution of the PDE, but it instead a genuine feature of the solution itself*. We believe that this is perhaps the most important result of this work, since it has concrete implications for numerical analysis and the numerical

solution of dispersive IVPs. Namely, when performing numerical simulations of dispersive PDEs, one must be very careful to distinguish among spurious Gibbs features induced by the truncation of a Fourier series representation, spurious Gibbs oscillations generated by numerical dispersion (introduced by the numerical scheme used to solve the PDE), and actual Gibbs-like behavior generated by the PDE itself.

7. The results of this work about the regularity of solutions bring up some interesting consequences. For example, if $q_o \in L^2(\mathbb{R}) \cap L^1((1+|x|)^\ell dx)$ is discontinuous where ℓ is large enough so that $q(x, t)$ is continuous for each t then the only discontinuity is at $t = 0$. Due to time reversibility, we know that $q(\cdot, t) \notin L^1((1+|x|)^\ell dx)$ for all $t \neq 0$ as this would imply that q_o is continuous. This is a clear illustration as to why L^1 -based spaces are not convenient for studying the well-posedness of these PDEs.

For example, whether there exist L^2 solutions that are never in $L^1(\mathbb{R})$ for all $t \in \mathbb{R}$. Or, equivalently, whether there is an L^2 solution of the PDE that is discontinuous at two different times. Also, an interesting question will be whether the results of this work can be extended to PDEs that are higher-order in time as well as PDEs in multiple spatial dimensions.

8. From a philosophical point of view, one may ask why consider PDEs with discontinuous ICs at all. In this respect we note on one hand that, apart from any physical considerations, studying these kinds of ICs is important from a mathematical point of view to understand the properties of the PDE and its solutions. Also, on the other hand, such a study also makes perfect sense physically. For example, one only need think about hyperbolic systems, for which considerable effort is devoted to the study of shock propagation. These shocks are discontinuities in the solution, and describe actual physical behavior. Even though such discontinuities are only approximation of a thin boundary layer, the fact remains nonetheless that representing such situations with discontinuous solutions is a convenient mathematical representation of the actual physical behavior. More in general, while the PDE holds in the interior of the domain $(x, t) \in \mathbb{R} \times \mathbb{R}^+$, the IC is posed on the *boundary* of this domain. In this sense $t = 0$ is always a singular limit. Indeed, the results of section 2 show that, generally speaking, the solution on the interior of the domain is smooth even when the IC is singular.

Appendix A. Brief review of well-posedness results

In this section we briefly review some well-known results about well-posedness of the IVP for the PDE (1.1) with dispersion relation (1.3) and IC (1.2).

We first show that the function $q(x, t)$ defined by the Fourier transform reconstruction formula (2.3) with $\theta(x, t, k) = kx - \omega(k)t$ is an L^2 solution of the IVP provided the imaginary part of $\omega(k)$ is bounded above and $q_o \in L^2(\mathbb{R})$. To see this, one can use the convolution property of the Fourier transform, which is a consequence of the Plancherel theorem: if $f, g \in L^2(\mathbb{R})$, then

$$(A.1) \quad \int_{\mathbb{R}} f(x)g(x)dx = \frac{1}{2\pi} \int_{\mathbb{R}} \hat{f}(k)\hat{g}(-k)dk.$$

Applying (A.1) (in x) to (2.2) yields

$$(A.2) \quad L_\omega[q, \phi] = \frac{1}{2\pi} \int_{\mathbb{R}^+} \int_{\mathbb{R}} e^{-i\omega(k)t} \hat{q}_o(k) (-i\partial_t \hat{\phi}(-k, t) - \omega(k) \hat{\phi}(-k, t)) dk dt.$$

But note that

$$-ie^{-i\omega(k)t} \hat{q}_o(k) \partial_t \hat{\phi}(-k, t) = -i\partial_t (e^{-i\omega(k)t} \hat{q}_o(k) \hat{\phi}(-k, t)) + \omega(k) e^{-i\omega(k)t} \hat{q}_o(k) \hat{\phi}(-k, t).$$

From this it follows that $L_\omega[q, \phi] = 0$ because of the compact support of ϕ .

We next show that the Fourier transform solution is unique. To see this, take $\phi(x, t) = X(x)T(t)$, for any L^2 solution we have

$$L_\omega[q, \phi] = \frac{1}{2\pi} \int_{\mathbb{R}} \hat{X}(-k) \int_{\mathbb{R}^+} \hat{q}(k, t) (-i\partial_t T(t) - \omega(k)T(t)) dt dk = 0.$$

Since the inner integral defines a locally integrable function (with polynomial growth) and X is arbitrary, the inner integral must vanish for a.e. k . Specifically, this follows from the density of $C_c^\infty(\mathbb{R})$ in the Schwartz class $\mathcal{S}(\mathbb{R})$. This is the weak form of an ODE for $\hat{q}(k, t)$ and we must show that the obvious solution of this is the only solution. We

rewrite this condition as (for fixed k)

$$(A.3) \quad 0 = -i \int_{\mathbb{R}^+} e^{i\omega(k)t} \hat{q}(k, t) (e^{-i\omega(k)t} T(t))_t dt.$$

Now, (A.3) implies that the integral of $e^{i\omega(k)t} \hat{q}(k, t)$ against any $C_c^\infty(\mathbb{R}^+)$ function with integral zero is zero: a $C_c^\infty(\mathbb{R}^+)$ function has integral zero iff it is the derivative of $C_c^\infty(\mathbb{R}^+)$ function. Now let $\phi, \psi \in C_c^\infty(\mathbb{R}^+)$ and choose ψ so that it integrates to one. Then

$$\phi(t) - \psi(t) \int_{\mathbb{R}^+} \phi(s) ds,$$

is a test function that integrates to zero. We find

$$\int_{\mathbb{R}^+} e^{i\omega(k)t} \hat{q}(k, t) \phi(t) dt = \int_{\mathbb{R}^+} \phi(s) ds \cdot \int_{\mathbb{R}^+} e^{i\omega(k)t} \hat{q}(k, t) \psi(t) dt,$$

and the inner integral in the right-hand side must be a constant $c(k)$ (independent of ψ). Thus

$$\int_{\mathbb{R}^+} [e^{i\omega(k)t} \hat{q}(k, t) - c(k)] \phi(t) dt = 0,$$

for all $\phi \in C_c^\infty(\mathbb{R}^+)$ and $e^{i\omega(k)t} \hat{q}(k, t) = c(k)$ is constant for a.e. t . This proves $\hat{q}(k, t) = e^{-i\omega(k)t} \hat{q}_0(k)$. Finally, examining (2.3), it is easily seen that the solution, as a function in $C^0([0, T]; L^2(\mathbb{R}))$ depends continuously on the initial data.

Appendix B. Asymptotics of the special functions and regularity results

In the first part of this section we concentrate on the steepest descent analysis of $I_{\omega, m}(x, t)$, which will also give us results concerning an important convolution kernel $K_t(x) \triangleq I_{\omega, -1}(x, t)$. Then in the last part of the section we apply these results to the IVP for the linear PDE (1.1).

We are interested in the asymptotics of $I_{\omega, m}(x, t)$ in two particular limits. First, in this section we need estimates for fixed t as $|x| \rightarrow \infty$. Estimates for fixed x as $t \rightarrow 0^+$ are also needed. For $|x| > 0$, $t > 0$, we rescale, by setting $\sigma = \text{sign}(x)$, $k = \sigma(|x|/t)^{1/(n-1)} z$

$$(B.1) \quad \begin{aligned} I_{\omega, m}(x, t) &= \frac{1}{2\pi} \sigma^m \left(\frac{|x|}{t} \right)^{-m/(n-1)} \int_C e^{X(iz - i\omega_n \sigma^n z^n - iR_{|x|/t}(z))} \frac{dz}{(iz)^{m+1}}, \\ R_{|x|/t}(z) &= \sum_{j=2}^{n-1} \omega_j \left(\frac{|x|}{t} \right)^{\frac{j-n}{n-1}} (\sigma z)^j, \quad X = |x| \left(\frac{|x|}{t} \right)^{1/(n-1)}. \end{aligned}$$

Here analyticity allows the deformation back to C (see Figure 3.1) after the change of variables.

The benefit of this scaling, as we will see, is that $R_{|x|/t}$ has coefficients that decay as $|x|/t$ increases. For $x < 0$ we perform a negative scaling to get it in a form where $X > 0$. This effectively maps ω_n to $\sigma^n \omega_n$ and because the lower-order terms in $R_{|x|/t}$ create lower-order effects the computation proceeds in the same way. Therefore, we provide all results for $x > 0$ noting the correspondence to $x < 0$. Define

$$\Phi_{|x|/t}(z) = iz - i\omega_n \sigma^n z^n - iR_{|x|/t}(z),$$

where $\{z_j\}_{j=1}^{n-1}$ are the roots of $\Phi'_{|x|/t}(z) = 0$ ordered counter-clockwise from the real axis. It is clear that there exists $n-1$ distinct roots for sufficiently large $|x|/t$ and such an ordering is possible.

Because it is the limiting case, consider $R_{|x|/t} \equiv 0$ (i.e. a monomial dispersion relation). We are interested in the roots of

$$n\omega_n \sigma^n z^{n-1} = 1.$$

- If n is even we have one root on the real axis and $(n-2)/2$ roots in the upper-half plane.
- If n is odd and $\omega_n \sigma^n$ is positive we have two roots on the real axis and $(n-3)/2$ roots in the upper-half plane.
- If n is odd and $\omega_n \sigma^n$ is negative we have no roots on the real axis and $(n-1)/2$ roots in the upper-half plane.

It is straightforward to check that for sufficiently large $|x|/t$ these statements hold for $\Phi'_{|x|/t}(z) = 0$. Define $N(n)$ to be this number of roots in the closed upper-half plane.

Consider the region $D = \{k : \text{Im } \omega_n \sigma^n k^n > 0\}$. This is the region in which $e^{-i\omega_n \sigma^n k^n}$ is unbounded and any contour deformation should avoid this region for large k . It is straightforward to check that D consists of n wedge-like sectors emanating from the origin. The steepest descent path through z_j satisfies

$$0 = \text{Im } \Psi_{|x|/t,j}(z), \quad \Psi_{|x|/t,j}(z) = \Phi_{|x|/t}(z) - \Phi_{|x|/t}(z_j).$$

Writing $z = re^{i\theta(r)}$ for large r we find

$$\cos(n\theta(r)) + O(r^{1-n} + r^{-1}(|x|/t)^{-1/n}) = 0.$$

Therefore using analyticity of the inverse cosine function near a zero of cosine

$$\theta(r) = \frac{2m+1}{2n}\pi + O(r^{-1}(1 + (|x|/t)^{-1/n})).$$

We note that the steepest descent directions of $e^{-i\omega_n \sigma^n k^n}$ are given by a subset of $\theta = \frac{2m+1}{2n}\pi$, $m = 0, \dots, 2n-1$ such that $\omega_n \sigma^n \sin n\theta > 0$. Thus, in this sense any unbounded portions of steepest descent paths are asymptotic, uniformly in $|x|/t$, to a steepest descent path of $e^{-i\omega_n \sigma^n k^n}$. We work towards understanding the paths of steepest descent that pass through $\{z_j\}_{j=1}^{N(n)}$. Next, we note that in the monomial case ($R_{|x|/t} \equiv 0$)

$$\text{Im}(iz_j - i\omega_n \sigma^n z_j^n) = \frac{n-1}{n} \text{Re } z_j.$$

Thus there can be path of steepest descent or ascent that connects to stationary points only if they have equal real parts. So, we compare their real parts:

$$(B.2) \quad \text{Re}(iz_j - i\omega_n \sigma^n z_j^n) = -\frac{n-1}{n} \text{Im } z_j.$$

It is clear that the exponent evaluated at stationary points in the upper-half plane has a smaller real part. Thus, any stationary point in the upper-half plane has no steepest descent path that connects to any other stationary point. Finally, it can be shown that the steepest descent path through z_j must be asymptotic to the closest (with respect to argument) steepest descent paths of $e^{-i\omega_n \sigma^n k^n}$. We establish the following:

Lemma B.1. *For sufficiently large $|x|/t$ there exists unique, disjoint contours $\Gamma_j \subset \{z : \text{Im } \Phi_{|x|/t}(z) = \text{Im } \Phi_{|x|/t}(z_j)\}$, $j = 1, \dots, N(n)$ such that*

- $z_j \in \Gamma_j$,
- Γ_j corresponds to the path of steepest descent from z_j , and
- Γ_j is asymptotic in each direction to a steepest descent path of $e^{-i\omega_n \sigma^n k^n}$.

Proof. Previous arguments demonstrate this in the monomial case. For the general case we note that $\{z_j\}$ converge to roots of $1 = n\omega_n \sigma^n z^n$ as $|x|/t \rightarrow \infty$ and the same conclusions follow. \square

From (B.2), in the monomial case, $z_j \in \overline{D}$. Furthermore, z_j and z_{j+1} lie in distinct sectors D_j and D_{j+1} of D and one and only one sector H_j of D^c lies between these two sectors (with counter-clockwise ordering). Let H_0 be the sector of D^c that lies before z_1 and $H_{N(n)}$ be the sector of D^c that lies after $z_{N(n)}$ with the same ordering. It is also clear that Γ_j cannot limit to infinity in any sector besides H_{j-1} and H_j as this would imply that the imaginary part of the exponent varied along the path. Next we understand the change of variables that is used along the steepest descent path.

It is important that Γ_j passes through one and only one stationary point z_j of the new exponent. Further, in the case that $R_{|x|/t} \equiv 0$ (i.e. a monomial dispersion relation) it is clear how to proceed: a straightforward application of the method of steepest descent for integrals will give the leading-order term. A derivation of the result in the general case requires some technical work. Define the variable $v_{|x|/t}(s)$ by the equation

$$\frac{\Psi_{|x|/t,j}(z_j + sv_{|x|/t})}{s^2} + 1 = 0, \quad v_{|x|/t}(0) = \pm(-\frac{1}{2}\Psi''_{|x|/t,j}(z_j))^{-1/2},$$

where \pm is chosen so that $\text{Re } \Psi_{|x|/t,j}(z_j + sv_{|x|/t}) \leq 0$. We use v_∞ to refer to the case where $R_{|x|/t} \equiv 0$. The Implicit Function Theorem can be applied for each $s \in \mathbb{R}$, producing the function $v_{|x|/t}(s)$ which depends smoothly on s and $|x|/t$ provided $|x|/t$ is sufficiently large, so that the coefficients of $R_{|x|/t}$ are sufficiently small. Applying the change of variables $k = \tau_{|x|/t}(s) = z_j + sv_{|x|/t}(s)$ we find

$$\int_{\Gamma_j} e^{X(iz - i\omega_n \sigma^n z^n - iR_{|x|/t}(z))} \frac{dz}{(iz)^{m+1}} = \int_{\mathbb{R}} e^{-Xs^2} \frac{\tau'_{|x|/t}(s)}{(i\tau_{|x|/t}(s))^{m+1}} ds.$$

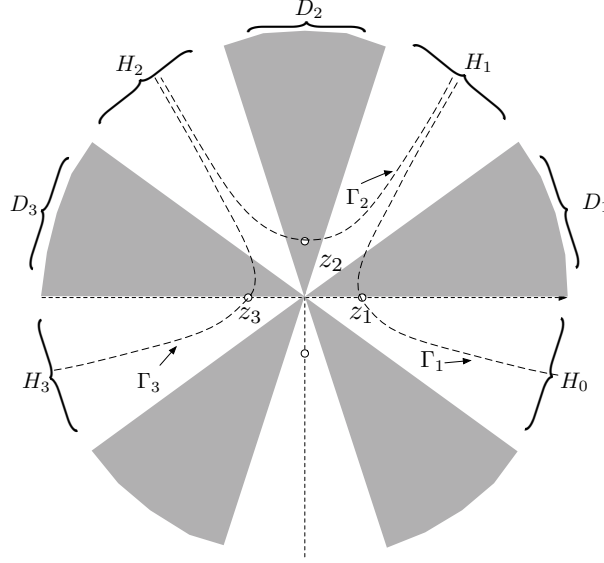


Figure B.1: A schematic for $\omega(k) = k^5 + O(k^4)$. The shaded region $S^c = \{z : \text{Im } \omega_n \sigma^n z^n > 0\}$ where the function $e^{-i\omega_n \sigma^n z^n}$ has growth. The circles represent the stationary points where $\Phi'_{|x|/t}(z) = 0$. The contours Γ_j which are along the global paths of steepest descent. This figure shows the definitions of the sectors H_j and D_j .

Now, one should expect that a Taylor expansion of

$$F_{m,|x|/t}(s) = \frac{\tau'_{|x|/t}(s)}{(i\tau_{|x|/t}(s))^{m+1}}$$

at $s = 0$ would produce a series expansion for the integral. But, because of the $|x|/t$ -dependence, extra work is required.

Lemma B.2. *There exists positive constants $C_{\ell,R}$ and $\varepsilon_{\ell,R}$ (depending only on ℓ , R and ω) such that for $|t/x| < \varepsilon_{\ell,R}$ and $|s| < R$*

$$\sup_{s \in \mathbb{R}} |F_{m,|x|/t}^{(\ell)}(s)| < C_{\ell,R}.$$

Proof. We begin by examining $v_{|x|/t}$ and its derivatives. First, because of the Implicit Function Theorem, $v_{|x|/t}(s)$ and all its derivatives depend continuously on s and $|x|/t$ for $|x|/t$ sufficiently large. Furthermore, all derivatives limit to v_∞ pointwise as $|x|/t \rightarrow \infty$. For every $s \in \mathbb{R}$ there exists ε_s such that for $|s' - s| < \varepsilon_s$ and $|t/x| < \varepsilon_s$,

$$|v_{|x|/t}^{(\ell)}(s') - v_\infty^{(\ell)}(s')| \leq |v_{|x|/t}^{(\ell)}(s') - v_\infty^{(\ell)}(s)| + |v_\infty^{(\ell)}(s) - v_\infty^{(\ell)}(s')| < \delta.$$

For $|s| \leq R$ we use compactness to cover $[-R, R]$ with a finite number of the balls $\{|s' - s_i| < \varepsilon_{s_i}\}$, and let $\varepsilon_{\ell,R} = \min_i \varepsilon_{s_i}$. It follows that for $|t/x| < \varepsilon_{\ell,R}$, and $|s| \leq R$ that $|v_{|x|/t}^{(\ell)}(s) - v_\infty^{(\ell)}(s)| < \delta$. \square

From previous considerations and the convergence of $v_{|x|/t}$ to v_∞ we have the following which is illustrated in Figure B.1.

Lemma B.3. *For sufficiently large $|x|/t$ and each $j = 1, \dots, N(n)$, z_j lies in a distinct sector $D_j \subset D$ and Γ_j tends to infinity in both H_{j-1} and H_j . Furthermore, H_j for $j = 2, \dots, N(n)-1$ contains unbounded components of two contours Γ_j and Γ_{j+1} , H_0 contains an unbounded component of Γ_1 and $H_{N(n)}$ contains an unbounded component of $\Gamma_{N(n)}$.*

This completes our characterization of the steepest descent paths and we consider the deformation of the integral.

Lemma B.4. *For $m \geq -1$*

$$\int_C e^{X\Phi_{|x|/t}(z)} \frac{dz}{(iz)^{m+1}} = \sum_{j=1}^{N(n)} e^{X\Phi_{|x|/t}(z)} \int_{\Gamma_j} \frac{dz}{(iz)^{m+1}},$$

where C is replaced with \mathbb{R} if $m = -1$.

Proof. We first work at the deformation of

$$\int_1^\infty e^{X\Phi_{|x|/t}(z)} \frac{dz}{(iz)^{m+1}}$$

off the real axis. It can be seen that the boundary of the sector H_0 contains the real axis. It follows from the fact that $\Phi_{|x|/t}(z)$ has purely imaginary coefficients there exists an interval $[c, \infty)$ that is a subset of the boundary of the region $S = \{z : \operatorname{Re} \Phi_{|x|/t}(z) \leq 0\}$ which may be above or below the real axis. Furthermore, the component of S whose boundary contains $[c, \infty)$ contains $\Gamma_1 \cap \{|z| > L\}$ for sufficiently large L and c can be taken to be independent of $|x|/t$. We justify the deformation of this integral to a contour that extends from 1 to one of the points in $\Gamma_1 \cap \{|k| = L\}$ and then follows Γ_1 for $|k| > L$. Call this contour Σ_1 , see Figure 2(b). To establish this it suffices to demonstrate that

$$(B.3) \quad \int_{C_R} e^{X(i\omega_n \sigma^n z^n - iR_{|x|/t}(z))} \frac{dz}{(iz)^{m+1}},$$

$$(B.4) \quad C_R = \{z : |z| = R, 0 \leq \pm \arg z \leq 1/(2n\pi) + O(R^{-1})\},$$

tends to zero for large R . The $+$, $-$ sign is taken if the deformation occurs above, below the real axis. Lemma B.1 demonstrates the asymptotic form of C_R . Since the integrand itself does not decay uniformly when $m = -1$ we perform integration by parts. Let $\gamma_R = \Gamma_1 \cap \{|k| = R\}$. Then

$$\begin{aligned} \int_{C_R} e^{X\Phi_{|x|/t}(z)} dz &= \frac{iX^{-1}}{n\omega^n \sigma^n z^{n-1} + R'_{|x|/t}(z)} e^{X\Phi_{|x|/t}(z)} \Big|_R^{\gamma_R} \\ &\quad + iX^{-1} \int_{C_R} \left(\frac{n(n-1)\omega^n \sigma^n z^{n-2} + R''_{|x|/t}(z)}{(n\omega^n \sigma^n z^{n-1} - R'_{|x|/t}(z))^2} - \frac{i}{n\omega^n \sigma^n z^{n-1} - R'_{|x|/t}(z)} \right) e^{X\Phi_{|x|/t}(z)} dz. \end{aligned}$$

The boundary terms here drop out in the large R limit. The non-exponential factor in the integrand decays at least like $1/z^2$ so that it suffices to show the exponential is bounded on C_R for sufficiently large R . This follows from the fact that for sufficiently large R , $C_R \subset S$. It is clear that the argument also holds for $m > -1$. Similar reasoning may be applied to

$$\int_0^\infty e^{X\Phi_{|x|/t}(z)} \frac{dz}{(iz)^{m+1}}$$

to justify a deformation to a segment of the contour Γ_2 . Call this deformed contours Σ_2 , again see Figure 2(b). Cauchy's Theorem justifies adding additional contour integrals, in the upper-half plane, which lie in S and, say, tend to a steepest descent direction of $e^{-i\omega_n \sigma^n k^n}$, see Figure B.3. The final step is to show that these additional contours can be joined with the original contour and deformed to $\cup_j \Gamma_j$. After some thought, it can be seen that it suffices to show that Γ_1 and Γ_2 can be deformed so that they connect with an added contour. The results of Lemmas B.1 and B.3 demonstrate this. See Figures 3(b) and 2(a) for a demonstration the deformation process. \square

We now consider the truncation of the integration domain.

Lemma B.5.

$$\int_{\Gamma_j} e^{X(i\omega_n \sigma^n z^n - iR_{|x|/t}(z))} \frac{dz}{(iz)^{m+1}} = \int_{\Gamma_j \cap \{|z| < R\}} e^{X(i\omega_n \sigma^n z^n - iR_{|x|/t}(z))} \frac{dz}{(iz)^{m+1}} + O(e^{-c_R X}),$$

where $c_R > 0$ is independent of $|x|/t$.

Proof. Consider

$$I_R = \int_{\Gamma_j \cap \{|z| \geq R\}} e^{X(i\omega_n \sigma^n z^n - iR_{|x|/t}(z))} \frac{dz}{(iz)^{m+1}},$$

and let $z = re^{i\theta(r)}$ on one of the components of $\Gamma_j \cap \{|z| \geq R\}$. Mirroring the calculations above $\theta(r) = \theta_0 + O(r^{-1})$ where θ_0 is a steepest descent direction for $e^{-i\omega_n \sigma^n k^n}$ and $\theta'(r) = O(r^{-1})$. Thus, $|dz| \leq Cdr$ and

$$B_R = \int_R^\infty \left| e^{X(-i\omega_n \sigma^n r^n (\cos(n\theta(r)) + O(r^{-1})))} \right| \frac{dr}{|r|^{m+1}} = \int_R^\infty e^{-X|\omega_n \sigma^n| r^n (1 + O(r^{-1}))} \frac{dr}{|r|^{m+1}}.$$

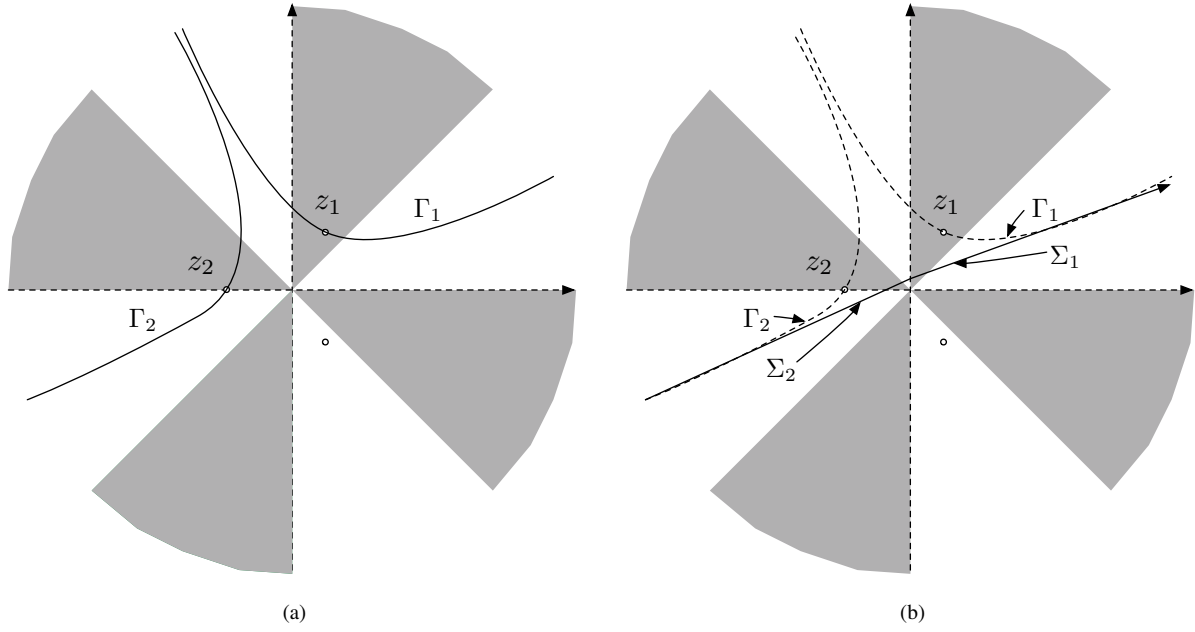


Figure B.2: A schematic for $\omega(k) = -k^4 + O(k^3)$. The shaded region $S^c = \{z : \text{Im } \omega_n \sigma^n z^n > 0\}$ where the function $e^{-i\omega_n \sigma^n z^n}$ has growth. The circles represent the stationary points where $\Phi'_{|x|/t}(z) = 0$. (a) The contours Γ_j which are along the global paths of steepest descent. (b) The initial deformation of the integral representation of $K_t(x)$, after scaling, to the contours Σ_1 and Σ_2 .

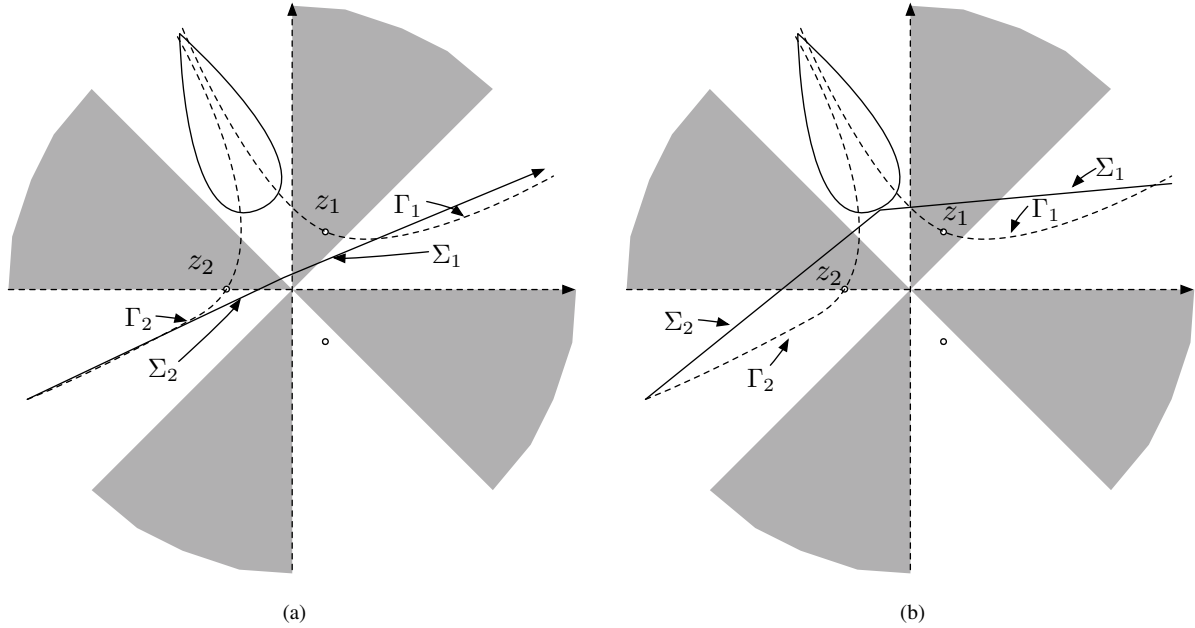


Figure B.3: A continuation schematic for $\omega(k) = -k^4$. The shaded region $S^c = \{z : \text{Im } \omega_n \sigma^n z^n > 0\}$ where the function $e^{-i\omega_n \sigma^n z^n}$ has growth. The circles represent the stationary points where $\Phi'_{|x|/t}(z) = 0$. (a) The addition of loop contours that contribute nothing (by Cauchy's Theorem) to the integral representation for $K_t(x)$. (b) The deformation of Σ_1 and Σ_2 to join with the loop contours. At this point it is clear that these contours may be deformed to $\Gamma_1 \cup \Gamma_2$.

Let R be large enough so that the $O(r^{-1})$ term is less than $1/2$ (uniformly for $|x/t|$ sufficiently large). Then

$$B_R \leq e^{-X|\omega_n \sigma^n| R^n / 4} \int_R^\infty e^{-X|\omega_n \sigma^n| r^n / 4} \frac{dr}{|r|^{m+1}} \leq C_{m,R} e^{-X|\omega_n \sigma^n| R^n / 4}.$$

From this we can conclude that for fixed m and fixed R , sufficiently large, $I_R = O(e^{-X|\omega_n \sigma^n| R^n / 4})$. \square

We are now prepared to complete the steepest descent analysis. Recall that

$$I_{\omega,m}(x, t) = \frac{1}{2\pi} \sum_{j=1}^{N(n)} \int_{\Gamma_j} \frac{e^{ikx - i\omega(k)t}}{(ik)^{m+1}} dk.$$

Theorem B.6. As $|x/t| \rightarrow \infty$

$$I_{\omega,m}(x, t) = -i \operatorname{Res}_{k=0} \left(\frac{e^{ikx - i\omega(k)t}}{(ik)^{m+1}} \right) \chi_{(-\infty, 0)}(x) + \frac{\sigma^m |x|^{-1/2}}{\sqrt{2\pi}} \left(\frac{|x|}{t} \right)^{-\frac{m+1/2}{n-1}} \sum_{j=1}^{N(n)} \frac{e^{X\Phi_{|x|/t}(z_j) + i\theta_j}}{(iz_j)^{m+1}} \frac{1}{|\Phi'_{|x|/t}(z_j)|^{1/2}} \left(1 + O \left(|x|^{-1} \left(\frac{|x|}{t} \right)^{-1/(n-1)} \right) \right).$$

Here θ_j is the direction at which Γ_j leaves z_j . Hence

- For fixed $t > 0$ as $|x| \rightarrow \infty$

$$(B.5) \quad K_t^{(m)}(x) \leq c \begin{cases} |x|^{\frac{2m-n+2}{2(n-1)}}, & n \text{ is even,} \\ |x|^{\frac{2m-n+2}{2(n-1)}}, & n \text{ is odd, } \omega_n x > 0, \\ |x|^{-M} \text{ for all } M > 0, & n \text{ is odd, } \omega_n x < 0, \end{cases}$$

where c depends on m, t and n .

- For $|x| \geq \delta > 0$ and $m \geq 0$ as $t \rightarrow 0^+$

$$(B.6) \quad I_{\omega,m}(x, t) = -i \operatorname{Res}_{k=0} \left(\frac{e^{ikx - i\omega(k)t}}{(ik)^{m+1}} \right) \chi_{(-\infty, 0)}(x) + O \left(t^{\frac{m+1/2}{n-1}} |x|^{-\frac{2m+2n}{2(n-1)}} \right).$$

Proof. We perform the steepest descent analysis of

$$L_{m,|x|/t}(X) = \int_{\Gamma_j \cap \{|z| < R\}} e^{X(iz - i\omega_n \sigma^n z^n - iR_{|x|/t}(z))} \frac{dz}{(iz)^{m+1}},$$

as X becomes large with $|x|/t \rightarrow \infty$. We assume R is chosen sufficiently large in the sense of Lemma B.5. We use the change of variables $k = \tau_{x/t}(s) = z_j + sv_{|x|/t}(s)$ to write

$$L_{m,|x|/t}(X) = \int_{c(R)_-}^{c(R)_+} e^{-Xs^2} F_{m,|x|/t}(s) ds = F_{m,|x|/t}(0) \int_{c(R)_-}^{c(R)_+} e^{-Xs^2} ds + F'_{m,|x|/t}(0) \int_{c(R)_-}^{c(R)_+} e^{-Xs^2} s ds + \frac{1}{2} \int_{c(R)_-}^{c(R)_+} e^{-Xs^2} s^2 F''_{m,|x|/t}(\xi(s)) ds.$$

Here $c(R)_\pm$ are chosen so that $|\tau_{|x|/t}(c(R)_\pm)| = R$. While these functions of R also depend on x and t , it is inconsequential because they tend to finite limit as $|x|/t \rightarrow \infty$. From Lemma B.2 the second integral is bounded by (assuming $c(R)_+ \geq c(R)_-$)

$$C \int_{|c(R)_-|}^{c(R)_+} e^{-Xs^2} s ds = O(e^{-X|c(R)_-|}).$$

Thus the error term is given by the third integral which by Lemma B.2 is $O(X^{-3/2})$. We find

$$L_{m,|x|/t}(X) = \sqrt{\pi} F_{m,|x|/t}(0) X^{-1/2} + O(X^{-3/2}).$$

We can confirm that the first term is indeed of higher-order because $F_{m,|x|/t}(0)$ as a definite limit as $|x|/t \rightarrow \infty$. Computing $F_{m,|x|/t}(0)$ explicitly and using (B.1) we find the result. \square

To clarify the various cases, in Figures B.4 and B.5 we show a schematic for $\omega(k) = k^5$ for $x > 0$. For $x < 0$, it suffices to consider $\omega(k) = -k^5$ with $x > 0$. Then all stationary points have non-zero imaginary parts and the shaded regions are switched with the unshaded regions.

We now are ready to prove the regularity theorem for linear dispersive equations, namely Theorem 2.4.

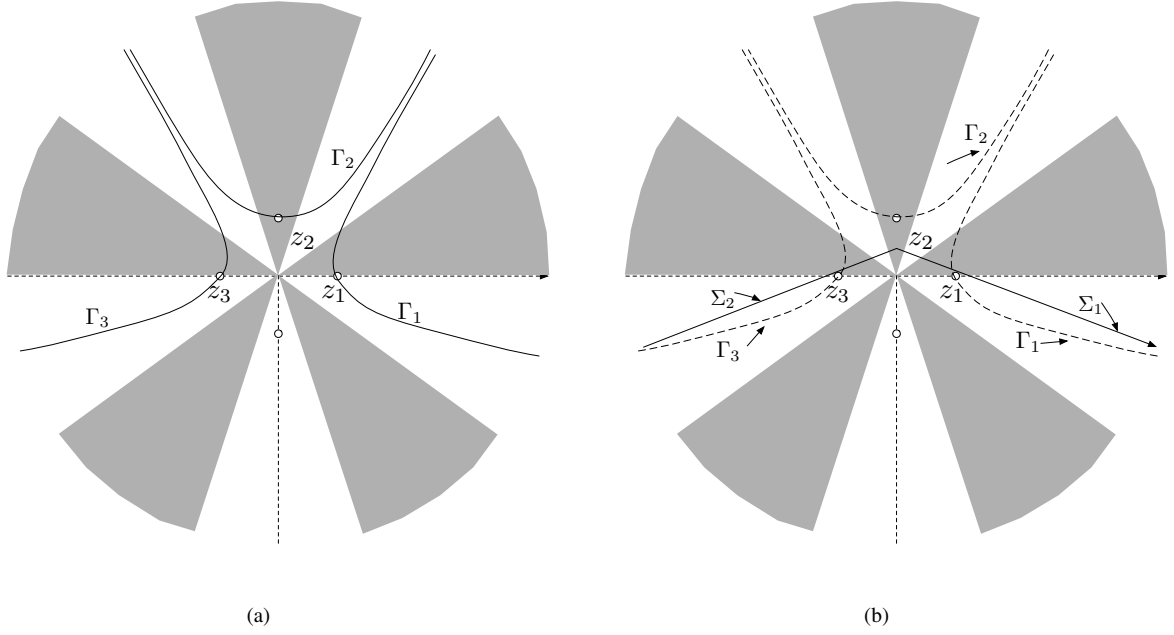


Figure B.4: A schematic for $\omega(k) = k^5$. The shaded region $S^c = \{z : \text{Im } \omega_n \sigma^n z^n > 0\}$ where the function $e^{-i\omega_n \sigma^n z^n}$ has growth. The circles represent the stationary points where $\Phi'_{|x|/t}(z) = 0$. (a) The contours Γ_j which are along the global paths of steepest descent. (b) The initial deformation of the integral representation of $K_t(x)$ to the contours Σ_1 and Σ_2 .

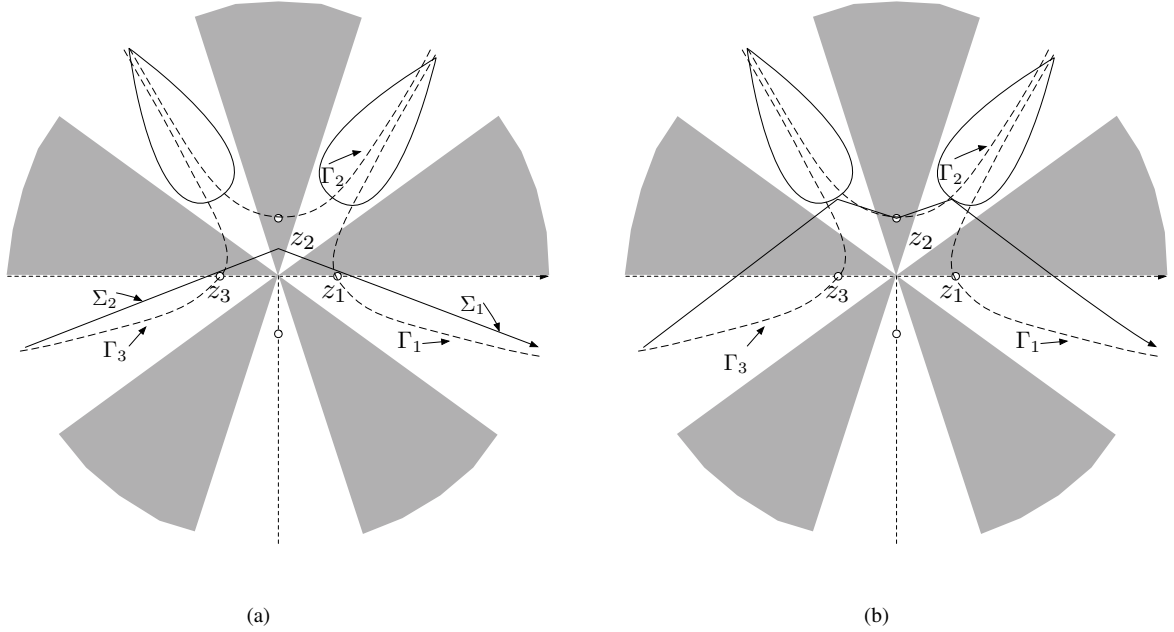


Figure B.5: A continuation schematic for $\omega(k) = k^5$. The shaded region $S^c = \{z : \text{Im } \omega_n \sigma^n z^n > 0\}$ where the function $e^{-i\omega_n \sigma^n z^n}$ has growth. The circles represent the stationary points where $\Phi'_{|x|/t}(z) = 0$. (a) The addition of loop contours that contribute nothing (by Cauchy's Theorem) to the integral representation for $K_t(x)$. (b) The deformation of Σ_1 and Σ_2 to join with the loop contours. At this point it is clear that these contours may be deformed to $\Gamma_1 \cup \Gamma_2 \cup \Gamma_3$.

Proof of Theorem 2.4. We write $q(x, t) = K_t * q_0(x)$. Because $q_0 \in L^2(\mathbb{R})$, the weak solution is given by this convolution. We must consider the convolution integral

$$(B.7) \quad q(x, t) = \int_{-\infty}^{\infty} K_t(x - y) q_0(y) dy.$$

Let B_x be a bounded open interval containing x . By Theorem B.6

$$|K_t^{(m)}(x - y) q_0(y)| \leq C \left(1 + |x - y|^{\frac{2m-n+2}{2(n-1)}}\right) (1 + |y|)^{-\ell} (1 + |y|)^{\ell} |q_0(y)|.$$

For $\ell \geq \frac{2m-n+2}{2(n-1)}$

$$\sup_{(x,y) \in B_x \times \mathbb{R}} C \left(1 + |x - y|^{\frac{2m-n+2}{2(n-1)}}\right) (1 + |y|)^{-\ell} = C_{\ell, B_x} < \infty.$$

This is sufficient to justify the differentiation under the integral (see [18, Theorem 2.27]). To see differentiability in t , we note that $\partial_t^j K_t(x)$ satisfies the same bounds, up to a constant, as $K_t^{(jn)}(x)$. \square

Recall that a direct consequence of Theorem 2.4 is Corollary 2.5 about the requirements on the IC to obtain a classical solution of the IVP.

Appendix C. Analysis of the residual

We now obtain estimates for the residual. Recall the decomposition (3.6), which we rewrite here for convenience:

$$(C.1) \quad q(x, t) = q_c + [q_0(c)] I_{0,\omega}(x - c, t) + q_{\text{res}}(x - c, t),$$

where

$$(C.2) \quad q_{\text{res}}(y, t) = \frac{1}{2\pi} \int_{\mathbb{R}} e^{ikc} \frac{e^{i\theta(y,t,k)} - 1}{ik} F(k) dk,$$

and $\theta(x, t, k)$ was defined in (2.4). It is trivial to see that $q_{\text{res}}(0, 0) = 0$.

Remark C.1. One must keep in mind that generically, $F \notin L^1(\mathbb{R})$. For if it was, then $\hat{q}'_o(k)$, defined on each interval of differentiability of \hat{q}_o , would be continuous. We did not require continuity in Assumption 3.1, so we have no reason to assume that such a condition would be satisfied. This fact complicates some of the estimates that follow.

We now want to show that $q_{\text{res}}(x - c, t)$ is continuous as $(x, t) \rightarrow (c, 0)$. We apply general arguments to analyze the behavior of as $(x, t) \rightarrow (c, 0)$ of

$$\int_{\mathbb{R}} e^{ikc} S_j(x - c, t, k) F(k) dk,$$

where

$$S_j(y, t, k) = \frac{1}{(ik)^{j+1}} \left(e^{i\theta(y,t,k)} - \sum_{r=0}^j a_r(y, t) k^r \right),$$

and where the $a_r(y, t)$ are the Taylor coefficients for $e^{i\theta(y,t,k)}$ at $k = 0$. To understand the behavior of these coefficients, we write [recalling (1.3)]

$$\theta(y, t, k) = ky + \sum_{j=2}^n \omega_j(k t^{1/j})^j.$$

We also note that $a_r(y, t)$ is expressible as a sum of terms of the form $y^{\beta_0} \prod_{i=1}^n t^{\beta_i/j}$, with $\sum_i \beta_i = r$. Taking $|x - c| \leq Ct$, then

$$(x - c)^{\beta_0} \prod_{i=1}^n t^{\beta_i/j} = O(t^{r/n}).$$

Thus we have $a_r(x - c, t) = O(t^{r/n})$ as $t \rightarrow 0$ with $|x - c| \leq Ct$.

We now use these results to estimate the $L^q(\mathbb{R})$ norm of $S_j(y, t, k)$. By Taylor's theorem, $S_j(y, t, k)$, on $[0, \alpha]$, is bounded by a polynomial of order $(n - 2)(j + 1)$ in α with coefficients that are of order $t^{(n-1)(j+1)/n}$. Thus for $\alpha > 1$

$$\left(\int_0^\alpha |S_j(k; x, t)|^q dk \right)^{1/q} \leq C t^{(n-1)(j+1)/n} \alpha^{(n-2)(j+1)+1/q}.$$

Furthermore

$$\left(\int_{\alpha}^{\infty} |S_j(k; x, t)|^q dk \right)^{1/q} \leq 2 \sum_{r=0}^j a_r(x-c, t) \alpha^{r-j-1+1/q}.$$

We note that when $\alpha = t^{-1/n}$ both integrals are of order $t^{(j+1)/n-1/(qn)}$. Therefore we obtain

Lemma C.1. *Suppose $F \in L^p(\mathbb{R})$ and $|x-c| \leq C|t|^n$ for $c \in \mathbb{R}$. Then*

$$\left| \int_{\mathbb{R}} e^{ikc} S_j(x-c, t, k) F(k) dk \right| \leq C_{p,j,\omega} t^{j/n+1/(np)} \|F\|_{L^p(\mathbb{R})}.$$

Remark C.2. *This lemma also allows the justification of an expansion of*

$$\int_{\mathbb{R}} e^{i\theta(x,t,k)} F(k) dk$$

about the point $(x, t) = (c, 0)$ when $F(\cdot)(1 + |\cdot|)^{j+1} \in L^2(\mathbb{R})$. Indeed,

$$\left| \int_{\mathbb{R}} e^{i\theta(x,t,k)} F(k) dk - \sum_{r=0}^j \int_{\mathbb{R}} \frac{a_r(x-c, t) k^r}{(ik)^{j+1}} (ik)^{j+1} F(k) dk \right| = \left| \int_{\mathbb{R}} e^{ikc} S_j(k; x, t) (ik)^j F(k) dk \right| \leq C_{j,\omega} t^{j/n+1/(2n)} \|F(\cdot)(1 + |\cdot|)^{j+1}\|_{L^2(\mathbb{R})}.$$

Appendix D. Approximation of ICs by smooth data

In this appendix we discuss the behavior of the solution of (1.1) with discontinuous data when it can be approximated, in an $L^1(\mathbb{R})$ sense, by smooth data.

Recall that, when the IC is continuous, the solution converges uniformly to it in the limit $t \downarrow 0$, and therefore it will not exhibit the Gibbs phenomenon as $t \rightarrow 0$. Nonetheless, we next show that, if the IC is a small perturbation of a discontinuous function, the solution exhibits Gibbs-like behavior *at finite times*. To see this, consider again the expression (B.7)

$$q(x, t) = \int_{-\infty}^{\infty} K_t(x-y) q_0(y) dy.$$

From (B.5) we know that, for $t > 0$, there exists $C_{m,\omega,t} > 0$ such that

$$|K_t^{(m)}(x)| \leq C_{m,\omega,t} (1 + |x|)^{\frac{2m-n+2}{2(n-1)}}.$$

Also, from Young's inequality we have for $|x| \leq R$, $R > 0$,

$$\begin{aligned} |\partial_x^m q(x, t)| &\leq C_{m,\omega,t,R} \|q_0\|_{L_{m,n}^1(\mathbb{R})}, \\ \|q_0\|_{L_{m,n}^1(\mathbb{R})} &\triangleq \int_{\mathbb{R}} |q_0(x)| (1 + |x|)^{\frac{2m-n+2}{2(n-1)}} dx, \end{aligned}$$

with a new constant $C_{m,\omega,t,R} > 0$. Now suppose one has a sequence $\{q_{o,\delta}\}_{\delta>0}$ of continuous ICs which converges to a discontinuous function q_o in the $L_{m,n}^1(\mathbb{R})$ norm as $\delta \downarrow 0$. Let $q_{\delta}(x, t)$ and $q(x, t)$ be the solution of (1.1) with initial data $q_{o,\delta}$ and q_o , respectively. It is straightforward to see that, for all fixed $t > 0$ and for all $j = 0, 1, \dots, m$,

$$(D.1) \quad |\partial_x^j(q(x, t) - q_{\delta}(x, t))| \rightarrow 0, \quad \delta \downarrow 0.$$

Equation (D.1) means that a *Gibbs-like phenomenon similar to the one arising for q as $t \downarrow 0$ will also be observed for q_{δ} at finite times, provided δ is sufficiently small*. Of course this statement does not hold uniformly as $t \downarrow 0$, because $C_{m,\omega,t} = O(t^{(-m-1/2)/(n-1)})$ as $t \downarrow 0$ (see (B.6)).

To illustrate these results, consider the following example, in which q_o is discontinuous at $x = \pm 1$ but the discontinuity at $x = -1$ is smoothed out in $q_{o,\delta}$:

$$(D.2) \quad q_o(x) = \begin{cases} 1, & |x| < 1, \\ 0, & \text{otherwise,} \end{cases} \quad q_{o,\delta}(x) = \begin{cases} (x+1+\delta)/\delta, & -1-\delta < x \leq 1, \\ 1, & |x| < 1, \\ 0, & \text{otherwise.} \end{cases}$$

Obviously $q_{o,\delta} \rightarrow q_o$ in any $L_{m,n}^1(\mathbb{R})$ norm. Also, the specific form of q_o and $q_{o,\delta}$ ensures that the corresponding solutions $q(x, t)$ and $q_{\delta}(x, t)$ are expressible in terms of the special functions $I_{\omega,m}$, and therefore can be computed to

arbitrary precision using the methods discussed earlier. The solution behavior is displayed in Figs. D.1 and D.2. While $q_\delta(x, t)$ converges uniformly to $q_{o,\delta}(x)$ near $x = -1$ as $t \downarrow 0$, $q(x, t)$ does not converge uniformly to $q_o(x)$ near $x = -1$ as $t \downarrow 0$. Nonetheless, for fixed $t > 0$, $q_\delta(x, t)$ converges uniformly to $q(x, t)$ near $x = -1$ as $\delta \rightarrow 0$.

Acknowledgements

We thank Mark Ablowitz, Bernard Deconinck, Pierre Germain and Nick Trefethen for interesting discussions related to this work. This work was partially supported by the National Science Foundation under grant numbers DMS-1311847 and DMS-1303018.

References

1. M J Ablowitz and H Segur, *Solitons and the inverse scattering transform* (SIAM, Philadelphia, 1981)
2. N. Bleistein and R. A. Handelsman, *Asymptotic expansions of integrals* (Dover, 1986)
3. G. Biondini and Y. Kodama, “On the Whitham equations for the defocusing nonlinear Schrödinger equation with step initial data”, *J. Nonlin. Sci.* **16**, 435–481 (2006)
4. J. P. Boyd and N. Flyer, “Compatibility conditions for time-dependent partial differential equations and the rate of convergence of Chebyshev and Fourier spectral methods”, *Comput. Methods Appl. Mech. Eng.* **175**, 281–309 (1999)
5. H. S. Carslaw, *Introduction to the theory of Fourier’s series and integrals* (Dover, 1930)
6. R. C. Y. Chin and G. W. Hedstrom “A Dispersion Analysis for Difference Schemes: Tables of Generalized Airy Functions”, *Math. Comp.* **32**, 1163–1170 (1978)
7. R. Courant and D. Hilbert, *Methods of mathematical physics* (Wiley, 1953)
8. P. Deift, S. Venakides, and X. Zhou, “The collisionless shock region for the long-time behavior of solutions of the KdV equation”, *Commun. Pure Appl. Math.* **47**, 199–206 (1994)
9. P. Deift and X. Zhou, “A steepest descent method for oscillatory Riemann-Hilbert problems. Asymptotics for the mKdV equation”, *Ann. Math.* **137**, 295–368 (1993)
10. J. C. DiFranco and K. T.-R. McLaughlin, “A nonlinear Gibbs-type phenomenon for the defocusing nonlinear Schrödinger equation”, *Int. Math. Res. Papers* **2005**, 403–549 (2005)
11. B. Dubrovin, “On Hamiltonian perturbations of hyperbolic systems of conservation laws, II: Universality of critical behavior”, *Comm. Math. Phys.* **267**, 117–139 (2006)
12. I. Egorova, Z. Gladka, V. Kotlyarov and G. Teschl, “Long-time asymptotics for the Korteweg-de Vries equation with step-like initial data”, *Nonlinearity*, **26**, 1839–1864 (2013)
13. G. A. El, V. V. Geogjaev, A. V. Gurevich, and A. L. Krylov, “Decay of an initial discontinuity in the defocusing NLS hydrodynamics”, *Physica D* **87** 186–192 (1995)
14. L. C. Evans, *Partial differential equations* (AMS, 2010)
15. N. Flyer and B. Fornberg, “Accurate numerical resolution of transients in initial-boundary value problems for the heat equation”, *J. Computat. Phys.* **184**, 526–539 (2003)
16. N. Flyer and B. Fornberg, “On the nature of initial-boundary value problems for dispersive equations”, *SIAM J. Appl. Math.* **64**, 546–564 (2003)
17. N. Flyer and P. N. Swarztrauber, “The convergence of spectral and finite difference methods for initial-boundary value problems”, *SIAM J. Sci. Comput.* **23**, 1731–1751 (2002)

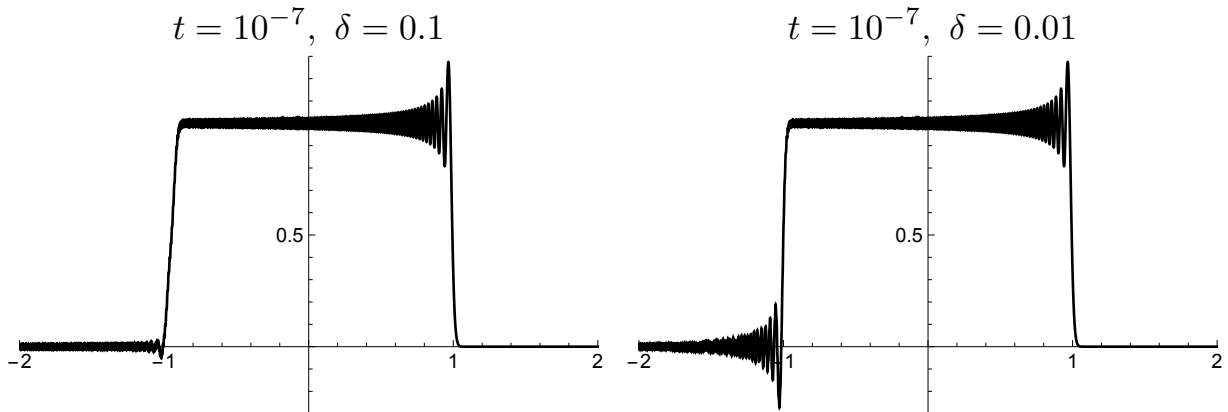


Figure D.1: The solution $q_\delta(x, t)$ with $\omega(k) = -k^3$ and IC (D.2) at $t = 10^{-7}$ for two different values of δ . Note how for $\delta = 0.1$ the Gibbs oscillations near $x = -1$ are absent, but $\delta = 0.01$ is sufficient for the solution to exhibit a Gibbs-like finite overshoot even at such extremely small values of time.

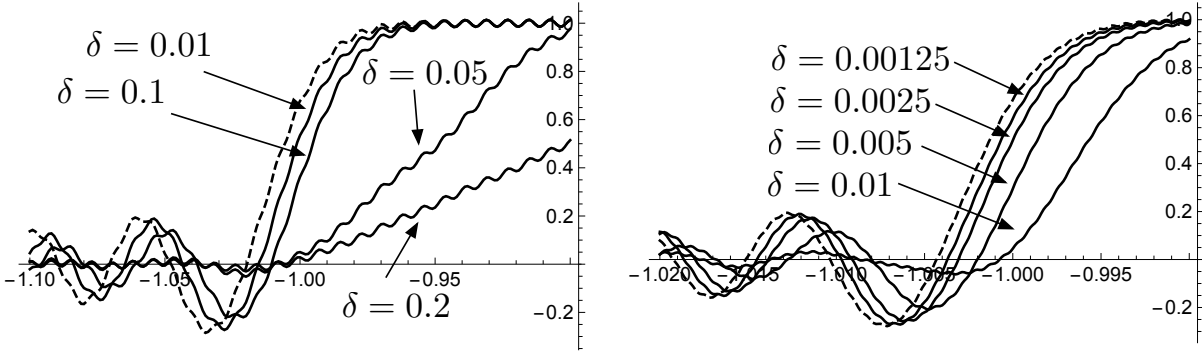


Figure D.2: The solutions $q(x, t)$ (dashed lines) and $q_\delta(x, t)$ (solid lines) with $\omega(k) = -k^3$ and ICs (D.2) at $t = 10^{-7}$ (left) and $t = 10^{-9}$ (right). Note how moderate values of δ make $q_\delta(x, t)$ a good approximation of $q(x, t)$ at small times.

18. G. B. Folland, *Real analysis* (Wiley, 1999)
19. A.S. Fokas, *A unified approach to boundary value problems* (SIAM, 2008)
20. J. W. Gibbs, "Fourier's Series" *Nature*, **59**, 200,606 (1899)
21. T. Grava and C. Klein, "Numerical solution of the small dispersion limit of Korteweg-deVries and Whitham equations", *Comm. Pure Appl. Math.* **60**, 1623–1664 (2007)
22. A. V. Gurevich and L. P. Pitaevskii, "Nonstationary structure of a collisionless shock wave", *Sov. Phys. JETP* **38**, 291–297 (1974)
23. E. Hewitt and R. E. Hewitt, "The Gibbs-Wilbraham Phenomenon: An Episode in Fourier Analysis", *Arch. for Hist. of Exact. Sci.* **21**, 129–160 (1979)
24. M. A. Hoefer, M. J. Ablowitz, I. Coddington, E. A. Cornell, P. Engels, and V. Schweikhard, "Dispersive and classical shock waves in Bose-Einstein condensates and gas dynamics", *Phys. Rev. A* **74** 023623 (2006)
25. A. M. Kamchatnov, *Nonlinear periodic waves and their modulations* (World Scientific, 2000)
26. S. Kamvissis, K. T. R. McLaughlin, P. D. Miller, *Semiclassical soliton ensembles for the focusing nonlinear Schrödinger equation*, Ann. Math. Stud., 154, (Princeton University Press, 2003)
27. C. E. Kenig, G. Ponce and L. Vega, "Oscillatory integrals and regularity of dispersive equations", *Indiana Univ. Math. J.* **40**, 33–69 (1991)
28. Y. Kodama, "The Whitham equations for optical communications: mathematical theory of NRZ", *SIAM J. Appl. Math.* **59**, 2162–2192 (1999)
29. V. Kotlyarov and A. Minakov, "Riemann-Hilbert problems and the mKdV equation with step initial data: short-time behavior of solutions and the nonlinear Gibbs-type phenomenon", *J. Phys. A* **45**, 325201 (2012)
30. N. Lebedev, *Special functions and their applications*, (Dover, 1972).
31. S. Lee, "On pointwise convergence of the solutions to Schrödinger equations in \mathbb{R}^2 ", *Int. Math. Res. Notices*, **2006**, 1–21 (2006)
32. S P Novikov, S V Manakov, L P Pitaevskii, and V E Zakharov, *Theory of solitons: The inverse scattering method* (Plenum, New York, 1984)
33. F. W. J. Olver, D. W. Lozier, R. F. Boisvert and C. W. Clark, *NIST Handbook of Mathematical Functions* (Cambridge, 2010)
34. S. Olver, "RHPackage: A Mathematica package for computing solutions to matrix-valued RiemannHilbert problems", <http://www.maths.usyd.edu.au/u/olver/projects/RHPackage.html>
35. P. Sjölin, "Regularity of solutions to the Schrödinger equation", *Duke Math. J.* **55**, 699–715 (1987)
36. T. Tao, *Nonlinear dispersive equations: Local and global analysis* (AMS, 2006)
37. T. Tao, "Low-regularity global solutions to nonlinear dispersive equations", in *Surveys in Analysis and Operator Theory*, CMA Proceedings, Canberra pp. 19–48 (2002)
38. T. Trogdon, *Riemann-Hilbert problems, their solution and the computation of nonlinear special functions*, Ph.D. thesis (University of Washington, 2013)
39. M. Taylor, "Short time behavior of solutions to nonlinear Schrödinger equations in one and two spatial dimensions", *Commun. PDE* **31**, 945–957 (2006)
40. L. Vega, "Schrödinger equations: Pointwise convergence to the initial data", *Proc. AMS* **102**, 874–878 (1988)
41. G. B. Whitham, *Linear and nonlinear waves* (Wiley, 1974)
42. H. Wilbraham, "On a certain periodic function", *Cambridge Dulin Math. J.* **3**, 198–201, (1848)

DEPARTMENT OF MATHEMATICS, STATE UNIVERSITY OF NEW YORK AT BUFFALO, BUFFALO, NY 14260

COURANT INSTITUTE OF MATHEMATIAL SCIENCES, NEW YORK UNIVERSITY, 251 MERCER ST., NEW YORK, NY, USA